Quaternary Research 83 (2015) 397–414

Contents lists available at ScienceDirect

Quaternary Research

journal homepage: www.elsevier.com/locate/yqres

Late Pleistocene deglaciation in the upper Gállego Valley, central Pyrenees

David Palacios [a,*], Nuria de Andrés [a], Juan I. López-Moreno [b], José M. García-Ruiz [b]

[a] Department of Geography, Universidad Complutense de Madrid, 28.040 Madrid, Spain
[b] Instituto Pirenaico de Ecología, CSIC, Campus de Aula Dei, P.O. Box 13.034, 50.080 Zaragoza, Spain

ARTICLE INFO

Article history:
Received 12 February 2014
Available online 7 March 2015

Keywords:
Deglaciation
Cosmogenic dating
Oldest Dryas
Bølling/Allerød
Younger Dryas
Central Pyrenees

ABSTRACT

Deglaciation processes in the upper Gállego Valley, central–southern Pyrenees, were studied using geomorphological mapping and ^{36}Cl cosmogenic dating of moraine and rock glacier boulders, as well as polished bedrock. Although the precise position of the Gállego Glacier during the global last glacial maximum is not known, there is evidence that ice tongues retreated to the headwaters, which caused subdivision of the main glacier into a number of individual glaciers prior to 17 ka. A range of ages (16 to 11 ka) was found among three tributary valleys within the general trend of deglaciation. The retreat rate to cirque was estimated to be relatively rapid (approximately 5 km per ka). The mapped glacial sedimentology and geomorphology appears to support the occurrence of multiple minor advances and retreats, or periods of stasis during the late deglaciation. Geomorphological and geological differences among the tributary valleys, and error estimates associated with the results obtained, prevented unambiguous correlations of the advances with the late Pleistocene cold periods. During the latter advances, small glaciers and rock glaciers developed close to the cirque headwalls, and co-occurred under the same climatic conditions. No evidence for Holocene re-advance was found for any of the three tributary valleys.

Introduction

The term 'last deglaciation' refers to the period between the global last glacial maximum (LGM) and the beginning of the Holocene (11.7 ka) (Darnault et al., 2012). The LGM can be defined as the global maximum ice volume recorded in the marine isotope records, and also by sea levels at approximately 23–19 ka. Peltier and Fairbanks (2006) dated the LGM at 26 ka, although it probably culminated at approximately 21 ka (Yokoyama et al., 2000; Mix et al., 2001). During the deglaciation period, the climate underwent a trend to warming interrupted by various cold, generally dry stadials that affected the extent of ice-sheets and valley glaciers (e.g. Combourieu-Nebout et al., 2009; Ballantyne, 2010; Fletcher et al., 2010). The study of deglaciation has focused on geomorphologically-derived aspects, such as the location and extent of glacial deposits during the various stadials, but also on climate aspects. Since the LGM, climate changes have been defined by their abrupt character, with sudden temperature increases and decreases that caused profound changes in vegetation distribution and landscape features in relatively short time periods (Combourieu-Nebout et al., 2009; Clark et al., 2012a). This highlights the instability of the Earth's environmental conditions, and the need to investigate paleoclimate shifts to enable detection of early warning signals in the immediate future (Scheffer et al., 2001; Lenton, 2011).

Studies of deglaciation in the northern hemisphere have been carried out in various locations including the Laurentide, Scandinavian and British-Irish ice sheets (Bowen et al., 2002; Scourse et al., 2009; Ballantyne, 2010; Williams et al., 2012; Ballantyne et al., 2013), valley glaciers of the Alps (Ivy-Ochs et al., 2004a, 2006, 2008, 2009; Kerschner and Ivy-Ochs, 2008; Ravazzi et al., 2012; Hippe et al., 2014), the Tatra Mountains and the Carpathians (e.g. Makos et al., 2013), and in Mediterranean mountains (Akçar et al., 2007, 2014; Zahno et al., 2009; Giraudi, 2012). Ivy-Ochs et al. (2004a) reported that the Rhône piedmont glacier collapsed at 21–19.1 ka. By 18 ka more than 80% of the ice volume of the alpine valley glaciers had disappeared. Deglaciation studies in the Iberian Peninsula have centered on the Sierra Nevada (Gómez-Ortiz et al., 2012), the Cantabrian Mountains (Moreno et al., 2010a,b, 2012; Pellitero et al., 2011; Rodríguez-Rodríguez et al., 2014), the Central Range (Palacios et al., 2011, 2012a,b), and both the Spanish (Jalut et al., 1992; González-Sampériz et al., 2006; Pallàs et al., 2006, 2010; Morellón et al., 2009; Moreno et al., 2012) and French (Bakalowicz et al., 1984; Jalut et al., 1992; Quinif and Maire, 1998; Delmas, 2005; Delmas et al., 2008, 2011, 2012; Calvet et al., 2011) sides of the Pyrenees. These studies have been based on marine and lake sediment analyses, including high resolution pollen analysis (González-Sampériz et al., 2006), U–Th dating of speleothems, and exposure dating using cosmogenic isotopes. These multi-proxy approaches have led to

* Corresponding author.
E-mail address: davidp@ucm.es (D. Palacios).

http://dx.doi.org/10.1016/j.yqres.2015.01.010
0033-5894/

relatively detailed knowledge of the various climatic pulses that occurred during the deglaciation period, represented by glacial advances and retreats. Nevertheless, many of the studies have lacked a detailed geomorphological approach, particularly those based on the analysis of marine and lake deposits. For instance, this was the case for the Pyrenees, where distinct cold and warm stages over the last 30,000 years were detected and dated using the Portalet peat-bog (González-Sampériz et al., 2006), for which a chronological model was constructed with the corresponding vegetation model; these stages included the Heinrich Event (HE) 2, LGM, HE1, Oldest Dryas, Bølling, Older Dryas, Allerød, Younger Dryas and the 8.2 event. There is no information on where the glacier fronts were located during the stadials and interstadials, or the rate of glacial retreat, even though geomorphological mapping has shown the distribution of the main tills in the Pyrenees (Chueca et al., 1998; García-Ruiz and Martí-Bono, 2002; García-Ruiz et al., 2011). Surprisingly, for several valleys there is much information on the location and dating of glacier fronts during the local maximum ice extent (MIE) of the last glacial cycle. Among these are the Cinca (Lewis et al., 2009), the Gállego (García-Ruiz et al., 2003), the Aragón (García-Ruiz et al., 2013), the Ariège (Delmas et al., 2011), the Têt (Delmas et al., 2008) and the Querol (Pallàs et al., 2010) valleys; the latter two studies included information on deglaciation stadials. Several methods, including optically stimulated luminescence (OSL) dating, cosmogenic exposure ages, U–Th series and ^{14}C, have been used to date deposits (tills and lacustrine sediments), stalagmite growth, and, in the case of cosmogenics, boulders deposited by glaciers and polished surfaces. Exposure age chronology has been used in dating glacial stages in the northern (Delmas et al., 2008, 2011) and eastern (Pallàs et al., 2010) Pyrenees, where it has contributed to identifying the occurrence of an early local MIE, distinguishing deposits of different ages over very short distance. This dating method has not previously been used in the central–southern Pyrenees, except for the Noguera Ribazgorzana Valley (Pallàs et al., 2006).

In this study we dated deglaciation in the upper Gállego Valley, based on exposure age chronology and geomorphological evidence; this is one of the most important and extensively studied valleys in the Pyrenees (Barrère, 1966; Serrano-Cañadas, 1991, 1998; Martínez de Pisón and Serrano, 1998; Julián et al., 2000; López-Moreno, 2000; García-Ruiz et al., 2003; Peña et al., 2003; González-Sampériz et al., 2006). Among these studies, mapping of the glacial deposits and landforms corresponding to distinct glacial periods has been conducted; few were dated, but those that were correspond to the local MIE. In this study, surface exposure ages were obtained from 6 moraine boulders, 8 rock glacier and paraglacial boulders and 7 polished bedrock surfaces in small valleys of the Panticosa massif, a granitic batholith located in the northeastern sector of the upper Gállego Valley (Fig. 1).

The main purpose of this study was to investigate deglaciation processes in the study area using analysis based on cosmogenic exposure dating (CED), including the retreat of glaciers and the occurrence of short advances with the deposition of new relatively recent tills, and to compare the results with those obtained elsewhere in the Pyrenees, the Iberian Peninsula and western Europe.

Local MIE and global LGM in the central–southern Pyrenees

Figure 2 shows the distribution of till deposits in the upper Gállego Valley, focusing on those belonging to the maximum expansion of the ice tongue. The local MIE is represented by several tills located between Biescas and Sabiñánigo (particularly the presence of dispersed boulders near Sabiñánigo), two small remnants in the mouth of the Aurín River, and the large terminal moraine of Senegüé (Barrère, 1966; Serrano-Cañadas, 1991, 1998; Peña et al., 2003; García-Ruiz et al., 2011). Lateral moraines (2–3) indicate the maximum ice development, with an ice thickness of approximately 400 m in the vicinity of Biescas and a substantial decrease in thickness towards Sabiñánigo. Many other tills representing the MIE are apparent upstream of Biescas. Using OSL dating techniques, Lewis et al. (2009) dated the end tills of Sabiñánigo, Aurín and Senegüé at 85 ± 5 ka, 64 ± 11 ka and 36 ± 3 ka, respectively, and showed good correspondence with the dates of fluvial terraces. González-Sampériz et al. (2006) also dated the MIE to earlier than 32–33 ka, based on sediments from the Portalet paleolake in the Gállego glacier headwalls. These dates are consistent with those obtained recently in the Aragón and Cinca valleys (Lewis et al., 2009; García-Ruiz et al., 2013), and in the eastern Pyrenees (Pallàs et al., 2010; Delmas et al., 2011, 2012), confirming the occurrence of a large glacial expansion during Marine Isotopic Stage (MIS) 4.

There is no clear evidence of the LGM in the Gállego Valley and neighboring Pyrenean valleys, as no tills of the global LGM have been found. Nevertheless, the LGM has been accurately identified in other Pyrenean valleys, including the Carol (Pallàs et al., 2010), Ariège (Jalut et al., 1992; Delmas, 2009) and Têt (Delmas et al., 2008; Delmas, 2009) valleys. A review by Calvet et al. (2011) includes a map showing the glaciated areas in the Pyrenees during the Würmian period. High-resolution multi-proxy analysis of the Portalet paleolake sediment enabled detection of the occurrence of a cold period involving glacial advance between 22,500 and 18,000 cal yr BP, during the global LGM (González-Sampériz et al., 2006). In addition, the base of a glaciolacustrine filling in a sinkhole near Búbal, 15 km upstream of the Senegüé moraine in the Gállego Valley, provided a ^{14}C age of 20,800 ± 400 yr BP (i.e. 25,928–23,182 cal yr BP) (Jalut et al., 1992), suggesting that the front of the Gállego glacier was located near the sinkhole during the LGM (Delmas, 2009). However, the Gállego glacier had retreated to the headwater by 20,150 ± 150 cal yr BP, as deduced from the occurrence of a large landslide and a dammed paleolake (the Corral de las Mulas peatbog) near the uppermost sector of the Gállego Valley (García-Ruiz et al., 2003).

Indirect evidence of a cold and geomorphologically active period has been found in the fluvial terraces of the Alcanadre River, between the Gállego and the Cinca river. Terrace Qt6 yielded an OSL age of 19 ± 2 ka, whereas Qt5 yielded an OSL age of 44 ± 2 ka (Calle et al., 2013). A cold and dry period was detected in a loess deposit in the Cinca Valley, with an OSL age of 20 ± 3 ka, and stratified screes located near the front of the MIE Cinca glacier gave an age of 22,800 ± 200 ^{14}C yr BP (27,490 cal yr BP; CALPAL) (García-Ruiz et al., 2001).

The study area

The upper Gállego Valley drains a large part of the central–southern Pyrenees (northeast Spain), and has a complex drainage area composed of various main and secondary valleys (Fig. 1). The study area is in the northeastern part of the basin, where the largest valleys and the highest peaks are located, including Balaitus (42°46′02 N, 0°15′02 W, 3151 m), Infierno (3082 m) and Argualas (3046 m). The Aguas Limpias and Caldarés valleys penetrate deeply into the highest reliefs, forming a series of tributaries that were occupied by cirques and glacial tongues. This headwater was selected because of the presence of a variety of tills corresponding to the glacial stades that followed the Würmian MIE. The presence of an extensive granitic batholith was also a factor in the selection of this area, as granite is associated with the occurrence of well-preserved polished surfaces and boulders, which are useful for cosmogenic sampling and analysis.

The upper Gállego Valley is composed of two of the main structural units of the southern Pyrenees: (i) the axial Paleozoic Pyrenees; and (ii) the south Pyrenean alpine fold and thrust belt. The former is composed of Silurian, Devonian, Ordovician and Carboniferous marine sediments, which were folded during the Hercynian tectonics (Carboniferous) and have schist, shale and limestone as the predominant materials. At the end of the Hercynian tectonics, two large granitic batholiths (Panticosa and Cauterets) were inserted through the already folded Paleozoic lithologies, causing the development of contacting metamorphic aureoles around the batholiths. Within the Paleozoic sector, limestone outcrops evolved towards small isolated massifs limited by cliffs, whereas shale outcrops developed large deep-seated landslides

https://doi.org/10.1016/j.yqres.2015.01.010 Published online by Cambridge University Press

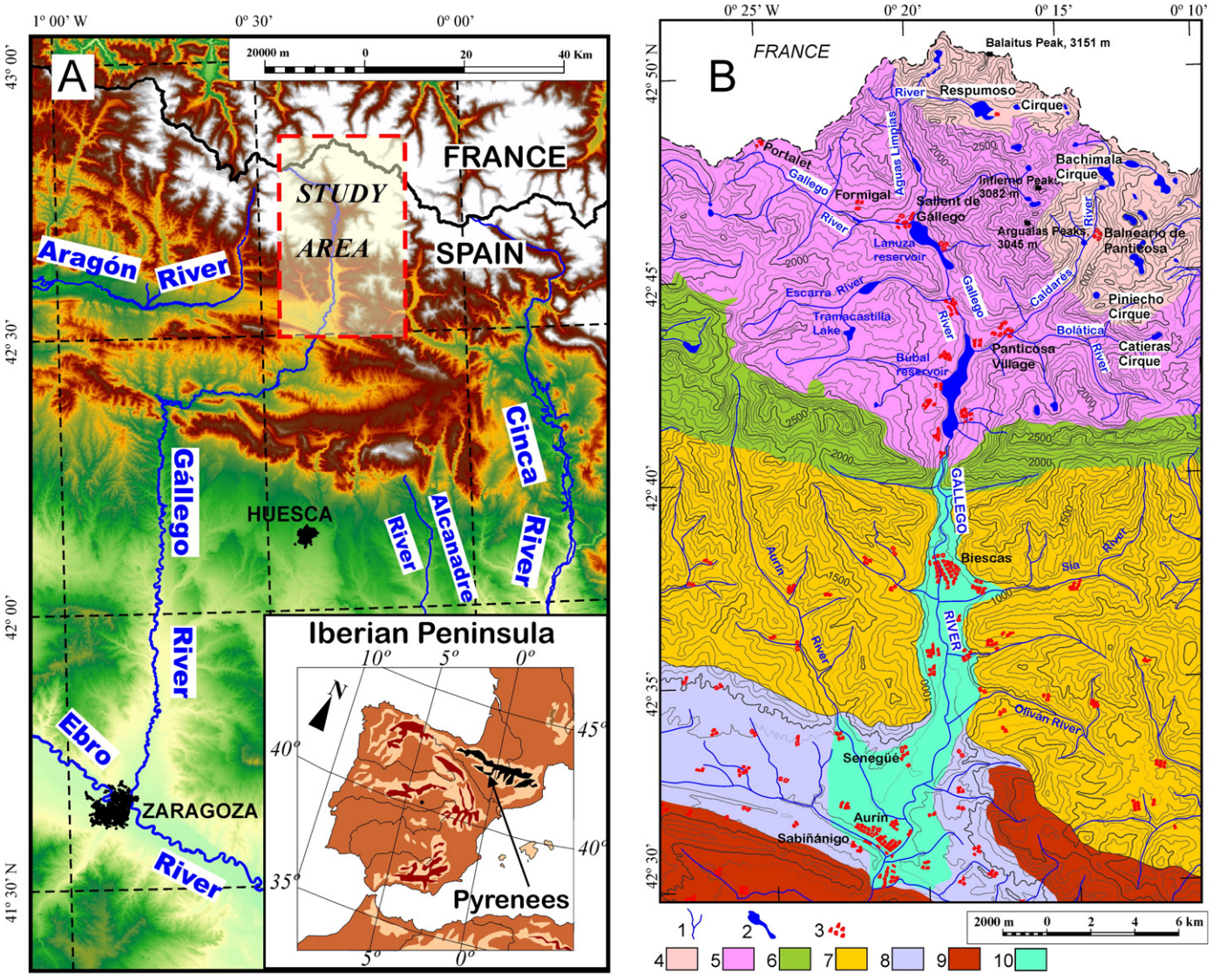

Figure 1. A: Location of the study area and main rivers cited in the text. B: The Alto Gállego Valley map, showing the main lithological outcrops and the valleys, cirques and peaks cited in the text. 1: Fluvial network. 2: Lakes and reservoirs. 3: Settlements. 4: Granites. 5: Paleozoic rocks. 6: Cenozoic limestone and sandstone. 7: Eocene flysch. 8: Eocene marl. 9: Oligocene sandstone and clay. 10: Quaternary deposits.

(Guerrero et al., 2013) that were related to deglaciation. The relief is characterized by wide and relatively smooth valleys having undulated slopes locally affected by badlands. The granitic batholiths evolved into high and steep massifs, with acute divides characterized by the presence of large, rounded, generally over-deepened glacial cirques occupied by lakes (García-Ruiz et al., 2000). Each valley accounts for several glacial troughs, developed at the confluence of two glacial valleys and delimited downstream by thresholds where the bedrock appears to be polished. Small-scale landforms are, in general, very well conserved.

The alpine Pyrenees is composed of marine Mesozoic and Cenozoic sediments, including Maastrichtian sandstone, and Cretaceous and Eocene limestones, forming a long and narrow ridge oriented from west to east: the so-called Inner Sierras. The Alpine tectonics resulted in stacking of a large south-verging overthrusting anticline, forming a dramatic vertical cliff on the north-facing slope, and complex structural reliefs on the south-facing slope, corresponding to the evolution of the front of the anticline.

The climate of the upper Gállego Valley is markedly influenced by Atlantic Ocean air masses, although a transition towards Mediterranean influences is evident. The study area receives average annual precipitation of >1200 mm, and >2000 mm above 2000 m asl. The precipitation gradient is 0.94 mm m^{-1} (de la Riva, 2000). The seasonal maximum precipitation occurs in winter, whereas the minimum occurs in summer. A consistent negative trend in snow accumulation in March and April has been observed since at least the middle of the 20th century (López-Moreno, 2005). The temperature gradient is 0.37°C 100 m^{-1} in January and December, and 0.54°C 100 m^{-1} in August (de la Riva, 2000). The 0°C isotherm in winter is located at 1611 m. The mean annual temperature is 6°C at Balneario de Panticosa (1620 m asl), 8°C at Lanuza (1283 m) and 9°C at Búbal (1150 m). Since the end of the Little Ice Age (LIA) a temperature increase of approximately 0.9°C has been estimated (López-Moreno, 2000).

Methods

A geomorphological survey of glacial forms and deposits was carried out in the upper Gállego Valley. The resulting geomorphological map was the basis for identifying the most suitable sites to sample for ^{36}Cl dating. Samples were collected (hammer and chisel) from moraine and rock glacier boulders > 1 m wide located on stable, gently sloping surfaces. Samples were also taken from areas: (i) of well-preserved glacial polish on bedrock steps, particularly at protruding sites, to reduce

https://doi.org/10.1016/j.yqres.2015.01.010 Published online by Cambridge University Press

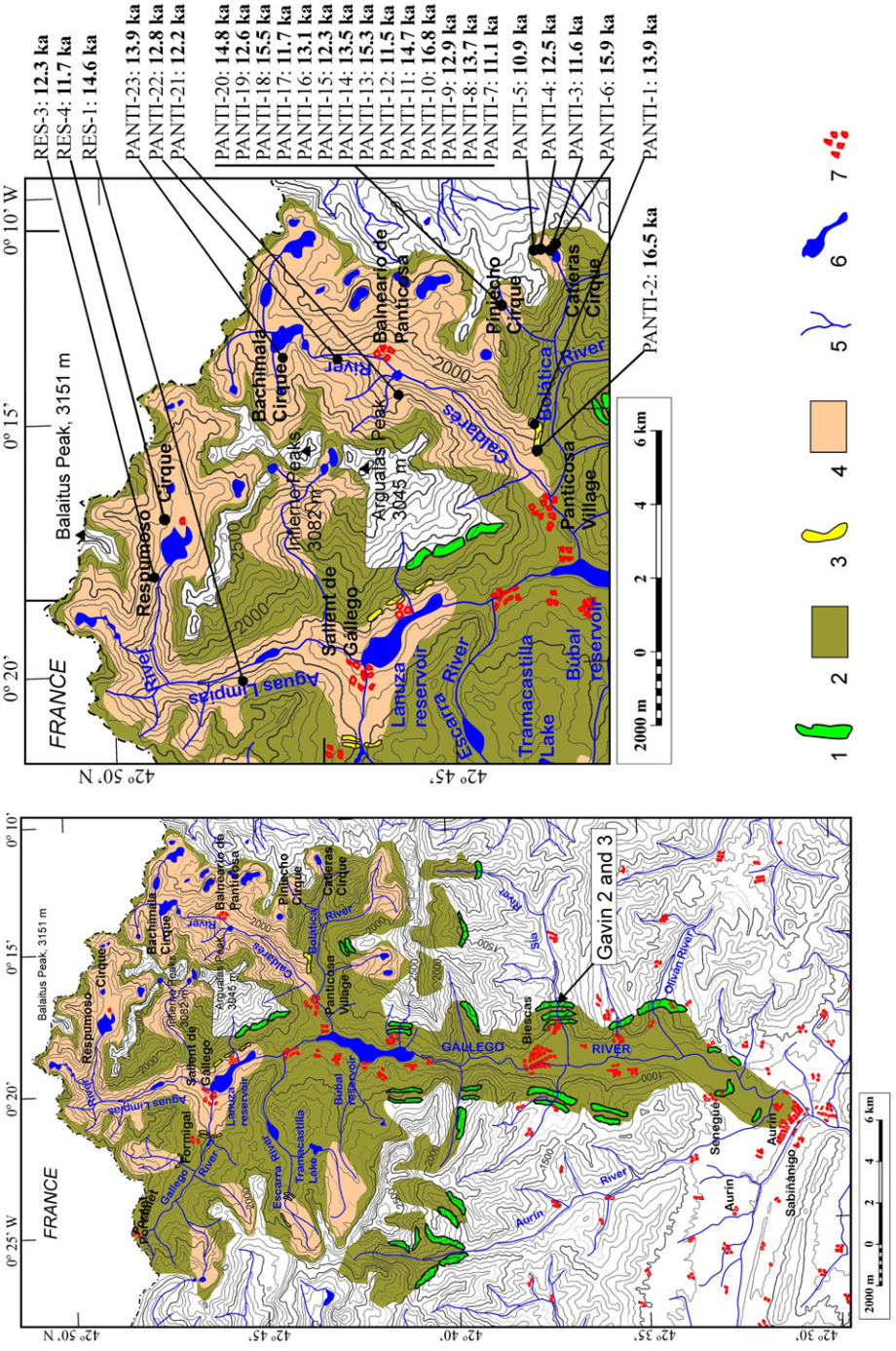

Figure 2. The extent of the Gállego Valley glacier during the maximum ice extent (MIE) and associated moraines, and the Aguas Limpias and Caldarés glaciers and associated moraines, with the cosmogenic results. 1: Moraines from the MIE. 2: Extent of the Gállego Glacier during the MIE. 3: Moraines from the readvance (Oldest Dryas?). 4: Maximum extent of the glaciers during this readvance. 5: Fluvial network. 6: Lakes and reservoirs. 7: Settlements.

https://doi.org/10.1016/j.yqres.2015.01.010 Published online by Cambridge University Press

the possibility of sediment cover and to minimize the effect of snow cover; (ii) of clear glacial polish, to ensure that the rock had not been eroded since deglaciation; and (iii) located where the former glacier was thick (thus maximizing erosion of the pre-glacial surface, and minimizing the chance of ^{36}Cl inheritance).

The study area is drained by the Aguas Limpias and Caldarés rivers, which are the two main tributaries of the Gállego River in its headwater. The five areas described below were selected for the sampling needed to investigate CED (Fig. 1).

(i) The Respumoso Cirque area, in the upper Aguas Limpias Valley. This is a wide valley in the headwater (Respumoso Lake), although it incises deeply into the granite downstream of the lake, forming a narrow canyon with some thresholds where polished granite occurs. The northern side of the valley received the ice tongues from the Balaitus massif, where a number of small glaciers remained until 25 years ago.
(ii) The Balneario de Panticosa resort area, in the upper Caldarés Valley. Between Balneario de Panticosa and Bachimaña Lake the valley is very steep, and includes several glacial troughs where polished and striated granite occurs at several points. No significant glacial tills have been found in this area, which has mainly been dominated by glacial erosion.
(iii) The lower Bolatica Valley, which is the main tributary of the Caldarés River. This valley contains glacial tills in its lower course. A large till is present on the left side of the valley, at approximately 400 m above the valley bottom. These deposits rest on a steep slope and are being intensively eroded, and so cannot be used to calculate the CED. Other deposits, located less than 100 m above the valley bottom, belong to a period of glacial advance or stabilization following the LGM, and were deposited by the glacial tongue of the Caldarés Valley. Some of these deposits rest on horizontal surfaces of thresholds and are very stable, and are therefore suitable for CED analysis.
(iv) The Catieras Cirque, in the upper Bolatica Valley. This is a glacial cirque developed on Devonian shale. The cirque tends to be rounded and remains perched 350 m above the main valley. A lake is located on the flat bottom of the cirque (which also has recent tills and a small rock glacier), far from the activity of the walls.
(v) The Piniecho Cirque, also in the upper Bolatica Valley. This is also a glacial cirque developed on granite bedrock. It contains a variety of very recent glacial deposits (rock glaciers; end and lateral moraines of different ages) within a small area, suggesting the occurrence of rapid climatic and geomorphological shifts. The moraine ridges and the front of the rock glacier rest on flat steps; they are not affected by the activity of the walls and are suitable for CED dating.
(vi) No suitable blocks for CED dating were found in lateral moraines from the MIE on the lateral slopes of the Gallego River, as the moraines are intensively eroded and/or covered by slope deposits. Only some blocks protrude, but they seem to have been exposed by agricultural activity.

We selected the ^{36}Cl cosmogenic nuclide because our research generally concerned the glacial chronology of different mountain areas, some of which do not have rocks suitable for analysis using other nuclides (e.g. ^{10}Be or ^{26}Al). In addition, other tributaries of the Gállego River are formed on limestone rocks, and the use of ^{36}Cl will enable comparative analyses of results in future studies. In addition, in areas where conditions are similar to those of our study the use of ^{36}Cl has yielded results that are consistent with those derived from ^{10}Be analysis (e.g. Phillips et al., 1997; Brugger, 2007).

The laboratory procedures for ^{36}Cl analysis in whole rock (Zreda et al., 1999; Phillips, 2003) were followed. Whole rock samples were crushed and pulverized using a roller grinder. Then they were sieved to separate the sand size fraction, and leached in deionized water and HNO_3 to remove atmospheric Cl. Next they were dissolved in a hot mixture of hydrofluoric and nitric acids, and $AgNO_3$ was added to the solution to precipitate AgCl. Sulfur was separated by precipitating $BaSO_4$. A spike of isotopically enriched ^{35}Cl was added during the dissolution process. This isotope dilution mass spectrometry method enabled the sample Cl content to be determined from accelerator mass spectrometry (AMS) analysis (Ivy-Ochs et al., 2004b; Desilets et al., 2006). The AMS analysis of the ^{36}Cl/Cl and ^{37}Cl/^{35}Cl ratios in the AgCl targets was carried out at the PRIME Laboratory (Purdue University, USA). The ^{36}Cl data is presented in Table 1.

Aliquots of rock, pre-treated (bulk rock) and post-treated (target fraction), were powered and analyzed for: (i) major elements, using fusion inductively coupled plasma optical emission spectrometry (ICP-OES); (ii) trace elements, using inductively coupled plasma mass spectrometry (ICP-MS); and (iii) boron, using prompt-gamma neutron activation analysis (PGNAA) at the Activation Laboratories (Ancaster, Canada). The element concentrations of bulk rock and target fraction are listed in Table 1.

The exposure ages were calculated using the spreadsheet for in-situ ^{36}Cl exposure age calculations proposed by Schimmelpfennig (2009) and Schimmelpfennig et al. (2009). We used the cosmogenic ^{36}Cl production rates for Ca spallation by Stone et al. (1996) (48.8 ± 3.4 atoms ^{36}Cl $(g\ Ca)^{-1}\ a^{-1}$) for K spallation by Schimmelpfennig et al. (2014) (148.1 ± 7.8 atoms ^{36}Cl $(g\ K)^{-1}\ a^{-1}$) for Ti spallation by Fink et al. (2000) (13 ± 3 atoms ^{36}Cl $(g\ Ti)^{-1}\ a^{-1}$), and for Fe spallation by Stone et al. (2005) (1.9 atoms ^{36}Cl $(g\ Fe)^{-1}\ a^{-1}$). The production rate of epithermal neutrons from fast neutrons in the atmosphere at the land/atmosphere interface by Phillips et al. (2001) (626 ± 46 neutrons $(g\ air)^{-1}\ a^{-1}$) was applied.

The "in situ" accumulation of ^{36}Cl depends on various factors including latitude, elevation, sample thickness, surrounding topography and snow cover. The elevation–latitude scaling factors for nucleonic and muonic production have been evaluated using CosmoCalc (Vermeesch, 2007), based on the scaling model of Stone (2000). The shielding factor has been calculated using the Topographic Shielding Calculator v1.0 of CRONUS-Earth Project (2014).

Snow cover (thickness and density) can under some circumstances reduce cosmogenic nuclide production rates in bedrock by up to ~15% (Benson et al., 2004; Schildgen et al., 2005). Recent studies, combining in situ ^{14}C and ^{10}Be dating methods, have demonstrated that partial surface shielding by snow has to be incorporated in the exposure age calculations and in models of deglaciation (Ivy-Ochs et al., 2009; Hippe et al., 2014). In the present study, many samples were collected from the valley bottom near summit areas, where substantial variation in snow cover occurs over very short distances because of factors including slope, aspect, wind redistribution and local topography variability. For the simplest case, we calculate the ages without considering the effect of the snow cover and for zero erosion rate of the boulder post glacial deposition. To estimate the numerical impact on exposure ages due to the effects of snow cover we calculated the snow shielding factor, applied the equation proposed by Gosse and Phillips (2001). The monitoring and simulations of snow cover in the upper Gallego Valley (1970–2000) revealed that snow cover lasts on average close to 80 days per year at 1500 m of altitude and 210 days per year at 2500 m (Lopez-Moreno et al., 2009). Snow depth at 2000 m of altitude is close to 1.5 m, with a response to temperature change of approximately 21% for every 1°C (López-Moreno et al., 2013). This sensitivity means that, assuming a lapse rate of 0.6°C every 100 m, snow depth should range between 50 and 250 cm from 1500 to 2500 m of altitude. These criteria were applied to evaluate the snow shielding factor. However, these numbers are subject to large variability even at very short scale (tens of meters) mainly due to aspect and convexity (López-Moreno et al., 2010). In order to face the effect of this large variability, the depth and duration of snowpack at each sampling site were

https://doi.org/10.1016/j.yqres.2015.01.010 Published online by Cambridge University Press

Table 1
Field and analytical data for ^{36}Cl samples from Gallego valley, Pyrenees, Spain.

Valley	Sample ID	Thickness	Sample mass	Mass of ^{35}Cl spike solution	Analytical stable isotope ratio	Analytical ^{36}Cl/Cl ratio	Measured ^{36}Cl concentration	Production rate (*)
		(cm)	(g)	(mg)	(^{35}Cl/(^{35}Cl + ^{37}Cl))	(^{36}Cl/10^{15} Cl)	(10^5 atoms ^{36}Cl g^{-1})	(atoms ^{36}Cl g^{-1} a^{-1})
Aguas Limpias	RES-1	1.5	30.02	1.041	7.59 ± 0.0550	87.67 ± 3.13	8.6 ± 0.5	5.6
	RES-3	2.5	30.19	1.035	3.92 ± 0.0160	192.69 ± 5.42	65.1 ± 2.8	50.0
	RES-4	2.0	30.17	1.044	4.12 ± 0.0190	211.81 ± 4.93	60.8 ± 2.2	47.1
Caldarés	PANTI-1	1.5	28.45	1.161	3.67 ± 0.0050	134.62 ± 3.48	74.0 ± 2.9	46.9
	PANTI-2	5.5	29.97	1.008	4.29 ± 0.0140	166.42 ± 6.63	40.2 ± 1.8	23.5
	PANTI-21	1.5	31.29	1.033	4.11 ± 0.0140	172.76 ± 4.39	47.3 ± 1.8	33.2
	PANTI-22	3.5	30.57	1.029	4.73 ± 0.0160	235.19 ± 5.72	45.9 ± 1.6	33.8
	PANTI-23	3.0	32.06	1.134	3.87 ± 0.0180	239.71 ± 5.73	90.2 ± 3.2	60.9
Piniecho	PANTI-7	2.5	30.29	1.071	4.00 ± 0.0120	210.93 ± 4.71	69.2 ± 2.3	60.3
	PANTI-8	5.0	30.41	1.030	4.03 ± 0.0150	254.85 ± 6.21	78.1 ± 2.8	54.8
	PANTI-9	2.5	30.01	1.058	3.66 ± 0.0080	195.75 ± 5.33	97.4 ± 3.9	69.5
	PANTI-10	5.0	30.18	1.047	3.77 ± 0.0100	194.02 ± 4.27	79.9 ± 2.6	46.1
	PANTI-11	6.0	29.97	1.058	3.57 ± 0.0630	176.28 ± 8.58	105.0 ± 14.7	67.1
	PANTI-12	5.0	31.61	1.037	3.99 ± 0.0160	193.51 ± 5.42	59.2 ± 2.4	49.3
	PANTI-13	4.0	31.90	1.118	3.82 ± 0.0240	237.24 ± 10.85	95.4 ± 5.4	60.0
	PANTI-14	4.0	31.12	1.025	3.83 ± 0.0100	226.14 ± 5.70	83.0 ± 3.1	58.1
	PANTI-15	5.5	30.03	1.024	3.99 ± 0.0100	224.15 ± 5.68	71.3 ± 2.6	53.7
	PANTI-16	4.0	30.07	1.018	3.82 ± 0.0010	174.95 ± 5.01	65.9 ± 2.8	48.9
	PANTI-17	2.5	30.05	1.022	3.84 ± 0.0300	170.86 ± 5.55	63.1 ± 3.0	51.4
	PANTI-18	3.5	31.57	1.080	4.23 ± 0.0090	279.04 ± 8.72	73.9 ± 3.3	46.2
	PANTI-19	5.0	30.46	1.010	4.20 ± 0.0190	222.17 ± 5.86	57.6 ± 2.2	42.8
	PANTI-20	5.0	30.27	1.124	4.21 ± 0.0100	248.65 ± 6.49	72.4 ± 2.8	46.8
Catieras	PANTI-3	2.0	31.36	1.048	5.16 ± 0.0150	249.29 ± 20.20	39.9 ± 3.5	33.0
	PANTI-4	3.0	30.72	1.082	4.73 ± 0.0210	267.16 ± 6.39	54.9 ± 1.9	42.9
	PANTI-5	3.5	30.70	1.026	4.64 ± 0.0230	248.08 ± 13.03	49.4 ± 2.8	42.2
	PANTI-6	3.0	30.17	1.097	7.76 ± 0.0170	315.23 ± 12.92	35.5 ± 2.1	22.3

(*) Scaled total sample specific ^{36}Cl production rate without radiogenic.

adjusted according with its specific location at the top of a boulder (convex) or at polished bedrock (plane or slightly concave). The snow shielding factor values resulted ranging from 0.86 to 0.97 among the samples. The snow cover value applied was based on snow conditions at the time of measurement. A factor not considered in the evaluation of our results was the different evolution of snow cover during the late Pleistocene and Holocene, which were periods of very short-term glacial change. In addition, we also included the change in age assuming a surface erosion rate of 3 mm/ka, which for all cases in this age range, resulted in an age decrease due to the subsurface ^{36}Cl maximum in production rate.

Results

The cosmogenic exposure results are summarized in Table 2 and Figure 3. All the parameters considered are included in the supplementary material. For cosmogenic dating of moraines corresponding to the maximum MIE (MIS 4) advances of the upper Gállego Valley glacier, moraine boulders on stable sites were selected for sampling according to the geomorphological map. A number of boulders were found on the oldest glacial deposits, but the surfaces had been affected by proglacial melt-out waters or hillslope processes, and none were undisturbed. However, the results for the boulder samples confirmed the field observations, suggesting that the boulders had been exhumed. For instance, the samples GAVIN-2 (42°36′44.802″N; 0°17′54.83″W) and GAVIN-3 (42°36′44.40″N; 0°17′53.89″W), from the outermost moraine, yielded ages of 5.3 ± 0.3 ka and 3.0 ± 0.4 ka, respectively. Consequently, these results were not included, and suggest that cosmogenic methods may not be suitable for dating the MIE and LGM stages in the upper Gállego Valley because of redistribution of boulders.

The first evidence of deglaciation was apparent upstream of the Búbal reservoir, where two tills indicated the occurrence of a stage during which the glacier was dissociated into two independent glacial tongues: the Aguas Limpias and the Caldarés glaciers (Serrano-Cañadas, 1991). At that time, only two of the three main valleys in the upper Gállego Valley (the Aguas Limpias and the Caldarés valleys) were occupied by ice tongues. The third, in the headwater of the Gállego Valley, was almost completely deglaciated because of the low altitude of the divides (<2300 m asl) relative to the other two valleys (>3000 m). The dissociation is demonstrated by the presence of lateral tills located at low altitude (<100 m above the valley bottom) in Lanuza (deposited by the Aguas Limpias glacier), and close to Panticosa, deposited by the Caldarés glacier in the lower course of its main tributary, the Bolatica Valley (Fig. 2). The presence of moraine ridges with granite blocks, which are oriented north to south at El Formigal, indicates that they were deposited by a glacier that came from the Aguas Limpias Valley. Consequently, the Gállego glacier was spatially restricted to higher altitudes. The Aguas Limpias glacier penetrated 2 km into the Gállego Valley, leaving the lateral moraines. Thus, the ice tongue of the Aguas Limpias glacier widened markedly, favoring a rapid decrease in thickness and melting of the glacier 3 km downstream of Sallent (Fig. 2).

All these moraines were unsuccessfully searched for boulders for sampling. Tills adjacent to the Lanuza and Búbal reservoirs are intensively disturbed by post-glacial erosion, and cannot be dated by cosmogenic methods. In addition, there are no thresholds having glacial polish, because the limestone and shale outcrops have been highly eroded.

However, in the middle and upper stretches of the Aguas Limpias Valley (Fig. 4), which is incised on granite, there are several glacial thresholds and troughs in the valley bottom. Three samples were collected from the best polished surfaces and dated: RES-1 (14.6 ± 2.3 ka), located at 1525 m asl.; RES-2 (11.7 ± 1.7 ka), located at 2132 m; and RES-3 (12.3 ± 1.6 ka), located at 2169 m near the cirque wall.

To analyze deglaciation in the tributaries of the upper Gállego River we collected samples from the Caldarés Valley, which is also on granitic substratum. A stable moraine was found at the confluence of the Caldarés River and its main tributary, the Bolatica River. The two more stable large protruding granite boulders on this moraine yielded a minimum age of 13.9 ± 2.0 ka (PANTI-01) (Fig. 5) and 14.6 ± 2.3 ka (PANTI-02).

The Caldarés Valley has similar characteristics to the Aguas Limpias Valley in having polished granitic thresholds in the valley bottom

https://doi.org/10.1016/j.yqres.2015.01.010 Published online by Cambridge University Press

Major elements concentration in bulk rock									
CaO (wt %)	K_2O (wt %)	TiO_2 (wt %)	Fe_2O_3 (wt %)	SiO_2 (wt %)	Na_2O (wt %)	MgO (wt %)	Al_2O_3 (wt %)	MnO (wt %)	P_2O_5 (wt %)
1.48	0.30	0.42	3.13	83.34	0.76	0.60	4.26	0.05	0.06
3.47	2.77	0.42	3.57	66.50	3.23	1.49	15.89	0.06	0.12
10.02	0.68	0.71	5.75	54.60	2.54	2.55	19.06	0.08	0.12
4.95	3.72	0.64	5.79	60.69	2.56	4.49	14.72	0.10	0.12
3.11	3.87	0.45	3.87	67.46	2.61	2.07	14.72	0.06	0.13
3.19	3.76	0.51	4.47	67.49	2.30	2.51	14.06	0.07	0.11
1.90	4.29	0.22	2.31	71.86	2.90	0.86	14.27	0.05	0.11
4.09	3.41	0.63	5.52	62.94	2.56	3.30	15.64	0.09	0.14
5.14	2.96	0.67	5.67	60.98	2.30	3.31	15.44	0.09	0.10
4.31	3.00	0.65	4.73	63.09	2.36	2.65	15.50	0.08	0.09
3.41	3.10	0.70	5.65	61.16	3.36	3.05	15.44	0.08	0.10
5.62	2.11	0.60	6.19	58.12	2.64	4.56	16.03	0.11	0.08
7.44	0.64	0.72	6.19	57.10	2.56	3.40	17.52	0.11	0.18
6.19	1.75	0.60	5.95	59.89	2.52	4.15	17.16	0.11	0.13
4.61	2.68	0.65	5.50	61.61	2.41	3.28	15.21	0.09	0.11
4.96	2.79	0.68	5.67	62.94	2.36	3.26	15.46	0.09	0.12
4.92	2.39	0.78	6.35	61.53	2.83	3.79	15.02	0.10	0.13
6.25	2.17	0.51	5.44	62.58	2.42	3.75	15.39	0.09	0.14
7.35	1.86	0.58	6.36	58.99	2.31	4.45	16.71	0.11	0.10
4.70	2.97	0.71	5.80	61.15	2.34	3.42	15.23	0.09	0.11
5.31	2.05	0.65	6.14	60.58	2.38	3.75	16.62	0.11	0.11
4.89	2.80	0.60	5.35	62.47	2.29	3.08	15.43	0.09	0.08
4.44	2.68	0.77	5.96	66.10	0.84	1.98	14.74	0.16	0.12
7.44	1.65	0.57	3.48	69.91	0.61	0.92	12.94	0.07	0.11
9.03	2.08	0.98	5.03	63.43	0.51	1.57	14.51	0.17	0.13
0.53	3.82	0.95	6.94	56.99	1.16	1.46	22.56	0.07	0.16

(Figs. 6 and 7). Three clear polished surfaces were sampled: one at Balneario de Panticosa, located at 1653 m (PANTI-21: 12.2 ± 1.5 ka); one at the front of the Bachimala Cirque, located at 1844 m (PANTI-22: 12.8 ± 1.4 ka); and one at the bottom of the Bachimala Cirque, located at 2218 m near the headwall (PANTI-23: 13.9 ± 1.8 ka).

The ages from moraines and thresholds in the Aguas Limpias and Caldarés Valley are very consistent and should be considered as minimum ages. Therefore, the results support the hypothesis that an important glacial advance occurred in the tributary valleys around 17–16 ka, but to obtain a precise timing for this advance is hampered by the large error rate. Following this advance the valleys were deglaciated, and were completely ice-free at approximately 12–14 ka ago.

The results suggest that the glaciers have not overstepped the base of the headwalls during the last 14 ka. To study the subsequent glacial evolution in these upper mountain areas, exposure ages were obtained in the Piniecho and Catieras glacial cirques, which are in tributaries of the Bolatica River.

The Piniecho cirque is composed of three cirques that had almost independent glacial development during the final deglaciation. It has a large variety of glacial-related deposits associated with valley tongues, small glaciers close to the cirque headwall, rock glaciers and a protalus lobe (Figs. 8 and 9). Figure 8 shows the geomorphological map of the Piniecho cirque, where six types of glacial deposit (described below) have been identified.

(i) The oldest deposit, based on its geomorphological position, is a large lateral moraine. The height of the moraine is 150 m high in the upper part, and this rapidly decreases downstream. The lower part of the moraine has disappeared, although it probably extended a further 350–500 m to the end of the glacier. This glacier would have had a total length of approximately 1500 m from the headwall, occupying two of the cirques and the main stem of the Piniecho Valley. The moraine ridge appears to have been interrupted by minor posterior glacial advances from the headwall. A very large granite block was sampled at 2319 m asl. (PANTI-18), and was found to have a ^{36}Cl exposure age of 15.5 ± 1.8 ka. The advance in the Piniecho Cirque must have been much more limited in extent than in the Aguas Limpias and Caldares valleys, as it was derived from mountains that were 500 m lower in altitude.

(ii) Following retreat of the Piniecho ice tongue, two small tongues developed from the northern and central cirques. The northern tongue was approximately 450–500 m in length, with a clear frontal end cut by a ravine, and the central tongue would have been approximately 700 m in length. No boulders suitable for cosmogenic exposure age analysis were available in any of the moraines, and consequently they have not been dated.

(iii) Two small rock or moraine-derived glaciers developed from the southern slope of the cirque. They are composed of various arcs and vallums. The innermost part of these rock glaciers is occupied by depressions containing small lakes and a chaotic rock avalanche. Two boulders were sampled in the upper part of the arcs in the western rock glacier: PANTI-16 (^{36}Cl exposure age of 13.1 ± 1.8 ka) and PANTI-17 (11.7 ± 1.7 ka). Three boulders were also sampled in the eastern rock glacier: PANTI-10 (16.8 ± 2.4 ka), PANTI-11 (14.7 ± 3.5 ka) and PANTI-12 (11.5 ± 1.5 ka). The differences in age between boulders within each of the rock glaciers may be related to later movement of the boulders. This could have occurred as a result of collapses because of later ice melting that caused displacement of the boulders.

(iv) A glacial advance from the headwall probably occurred contemporaneously with development of the rock glaciers. This advance caused the formation of a wavy moraine corresponding to two small ice tongues. Two boulders were sampled on the ridge of this moraine (PANTI-13: 15.3 ± 2.3 ka; and PANTI-14: 13.5 ± 1.8 ka). Another boulder (PANTI-15: 12.3 ± 1.7 ka) was sampled in a relatively isolated body of the moraine, which apparently developed in a later period. Inheritance is possibly the reason for the inconsistent exposure age

https://doi.org/10.1016/j.yqres.2015.01.010 Published online by Cambridge University Press

Table 1 (*continued*)

Valley	Trace elements concentration in bulk rock					Element concentration in target fraction				
	B (ppm)	Sm (ppm)	Gd (ppm)	Th (ppm)	U (ppm)	CaO (wt %)	K_2O (wt %)	TiO_2 (wt %)	Fe_2O_3 (wt %)	Cl (ppm)
Aguas Limpias	17.60	4.10	3.10	7.00	1.60	0.96	0.30	0.43	3.16	31.48
	5.50	4.60	2.90	8.30	3.20	3.50	2.80	0.40	3.37	175.12
	4.60	3.30	2.80	5.80	1.80	9.87	0.69	0.69	5.73	142.66
Caldarés	6.50	5.30	4.20	11.00	1.70	4.86	3.79	0.62	5.67	305.05
	44.20	4.70	3.50	11.10	1.90	3.13	3.73	0.36	3.00	110.70
	5.90	3.80	3.40	11.70	5.20	3.22	3.53	0.45	3.89	136.97
	7.20	3.50	2.70	10.50	2.80	1.74	3.98	0.19	1.88	85.71
	8.10	5.90	4.20	13.30	1.90	3.91	3.40	0.64	5.19	193.71
Piniecho	19.30	5.50	4.20	7.00	1.50	5.62	2.75	0.52	4.73	165.72
	29.80	4.60	3.30	13.30	2.00	4.16	2.99	0.59	4.29	152.47
	10.80	4.50	3.60	10.10	2.20	1.26	3.16	0.69	5.50	269.51
	25.40	4.20	3.10	6.90	1.20	5.63	2.19	0.60	6.03	218.37
	12.90	5.40	4.10	7.60	1.70	7.21	0.66	0.71	5.99	317.00
	36.00	5.10	3.70	7.70	1.80	6.20	1.61	0.51	5.45	155.60
	19.40	5.90	4.40	12.30	1.10	4.86	2.44	0.50	4.56	200.80
	18.80	5.10	4.20	12.10	2.00	5.08	2.59	0.52	4.52	190.91
	11.90	6.50	4.90	12.20	3.10	4.47	2.28	0.70	5.56	160.31
	44.20	4.90	3.70	8.00	1.30	6.50	1.83	0.37	4.55	199.27
	22.50	4.70	3.80	7.00	1.60	7.84	1.28	0.36	4.80	195.09
	27.60	4.90	3.70	10.20	2.70	4.69	2.95	0.67	5.37	126.45
	11.80	6.50	4.80	11.90	2.00	5.14	2.02	0.57	5.51	125.72
	10.60	5.70	4.30	12.10	1.30	5.09	2.70	0.51	4.63	140.23
Catieras	23.70	10.30	7.80	20.80	3.10	4.28	2.74	0.82	6.03	59.40
	23.90	6.80	5.50	12.50	2.00	7.44	1.67	0.59	3.39	89.80
	31.00	14.00	10.70	31.80	5.00	8.64	2.09	0.97	4.70	82.50
	84.20	12.10	8.80	22.50	3.00	0.40	3.88	1.00	6.94	31.76

of PANTI-10 and PANTI-13, because of their proximity to the headwall (570 and 600 m).

(v) At the foot of the southern cirque there is a relatively complex lobate protalus lobe related to rock avalanches; this has various ridges that show an initial trend towards a rock glacier. Three boulders were sampled at this site: PANTI-7 (11.1 ± 1.3 ka), PANTI-8 (13.7 ± 1.7 ka) and PANTI-9 (12.9 ± 2.1 ka).

(vi) A rock glacier developed in the western sector of the Piniecho Cirque area, and has several arcs composed of large boulders. The rock glacier is derived directly from a scarp in the valley wall, and probably formed following retreat of the main ice tongue of the Piniecho cirque. Two boulders were sampled on the ridges: PANTI-19 (12.6 ± 1.6 ka) and PANTI-20 (14.8 ± 1.9 ka).

Table 2
^{36}Cl exposure ages, sample type and sample location. Ages are reported for 0 mm/ka erosion rate. Errors correspond to the analytical uncertainty of the AMS ^{36}Cl determination (one standard deviation). Ages are also reported for snow shielding and 0 mm/ka erosion rate and snow shielding and 3 mm/ka erosion rate.

Valley	Sample	Sample type	Distance from the headwall	Latitude	Longitude	Elevation	Topography correction factor	Zero erosion age	Snow correction factor	Age with snow correction and zero erosion	Age with snow correction and 3 mm ka^{-1} erosion
	ID		(m)	°N (DD)	°W (DD)	(m)	(unitless)	(ka)	(unitless)	(ka)	(ka)
Aguas Limpias	RES-1	Polished bedrock	8600	42.8090	0.3391	1525	0.92	**14.6 ± 2.3**	0.97	14.8 ± 2.3	13.6 ± 2.2
	RES-3	Polished bedrock	2600	42.8167	0.2957	2132	0.93	**11.7 ± 1.7**	0.86	12.5 ± 1.9	11.7 ± 1.8
	RES-4	Polished bedrock	2400	42.8139	0.2785	2169	0.97	**12.3 ± 1.6**	0.86	13.2 ± 1.8	12.3 ± 1.7
Caldarés	PANTI-1	Moraine boulder	11,800	42.7218	0.2462	1519	0.93	**13.9 ± 2.0**	0.97	14.1 ± 2.1	13.1 ± 1.9
	PANTI-2	Moraine boulder	11,700	42.7235	0.2606	1442	0.88	**16.5 ± 1.8**	0.97	16.8 ± 1.8	16.7 ± 1.8
	PANTI-21	Polished bedrock	7300	42.7550	0.2397	1653	0.93	**12.2 ± 1.5**	0.97	12.4 ± 1.5	11.8 ± 1.4
	PANTI-22	Polished bedrock	6000	42.7671	0.2305	1844	0.96	**12.8 ± 1.4**	0.94	13.3 ± 1.5	13.0 ± 1.4
	PANTI-23	Polished bedrock	3075	42.7890	0.2308	2218	0.98	**13.9 ± 1.8**	0.86	14.9 ± 2.1	14.0 ± 2.0
Piniecho	PANTI-7	Rock glacier boulder	395	42.7284	0.2082	2434	0.96	**11.1 ± 1.3**	0.86	12.0 ± 1.5	11.5 ± 1.5
	PANTI-8	Rock glacier boulder	395	42.7284	0.2082	2429	0.93	**13.7 ± 1.7**	0.86	14.8 ± 1.9	14.3 ± 1.8
	PANTI-9	Rock glacier boulder	405	42.7288	0.2081	2425	0.93	**12.9 ± 2.1**	0.86	13.6 ± 2.3	12.6 ± 2.1
	PANTI-10	Moraine boulder	600	42.7286	0.2120	2374	0.70	**16.8 ± 2.4**	0.86	17.9 ± 2.7	16.9 ± 2.5
	PANTI-11	Moraine boulder	635	42.7299	0.2112	2356	0.82	**14.7 ± 3.5**	0.86	15.2 ± 3.7	14.1 ± 3.4
	PANTI-12	Moraine boulder	600	42.7295	0.2111	2353	0.99	**11.5 ± 1.5**	0.86	12.4 ± 1.7	12.0 ± 1.6
	PANTI-13	Moraine boulder	570	42.7297	0.2100	2370	0.95	**15.3 ± 2.3**	0.86	16.3 ± 2.5	15.4 ± 2.4
	PANTI-14	Moraine boulder	530	42.7304	0.2090	2397	0.90	**13.5 ± 1.8**	0.86	14.5 ± 2.1	14.5 ± 2.1
	PANTI-15	Moraine boulder	555	42.7311	0.2093	2382	0.94	**12.3 ± 1.7**	0.86	13.1 ± 1.9	12.6 ± 1.8
	PANTI-16	Rock glacier boulder	405	42.7303	0.2138	2273	0.91	**13.1 ± 1.8**	0.86	14.0 ± 2.0	13.4 ± 1.9
	PANTI-17	Rock glacier boulder	415	42.7298	0.2150	2291	0.92	**11.7 ± 1.7**	0.86	12.4 ± 1.9	11.8 ± 1.8
	PANTI-18	Moraine boulder	940	42.7311	0.2118	2319	0.90	**15.5 ± 1.8**	0.86	17.0 ± 2.0	16.4 ± 2.0
	PANTI-19	Rock glacier boulder	530	42.7319	0.2181	2209	0.95	**12.6 ± 1.6**	0.86	13.6 ± 1.8	13.1 ± 1.8
	PANTI-20	Rock glacier boulder	555	42.7321	0.2182	2212	0.89	**14.8 ± 1.9**	0.86	16.0 ± 2.1	15.2 ± 2.0
Catieras	PANTI-3	Rock glacier boulder	450	42.7221	0.1973	2308	0.86	**11.6 ± 1.4**	0.86	13.0 ± 1.6	12.9 ± 1.6
	PANTI-4	Rock glacier boulder	430	42.7228	0.1975	2322	0.99	**12.5 ± 1.3**	0.86	13.7 ± 1.5	13.3 ± 1.5
	PANTI-5	Moraine boulder	670	42.7230	0.1993	2337	0.91	**10.9 ± 1.2**	0.86	12.1 ± 1.3	12.1 ± 1.3
	PANTI-6	Polished bedrock	800	42.7189	0.1971	2295	0.76	**15.9 ± 1.6**	0.86	18.5 ± 1.9	18.5 ± 1.9

Bold values indicate the date considered in the text.

https://doi.org/10.1016/j.yqres.2015.01.010 Published online by Cambridge University Press

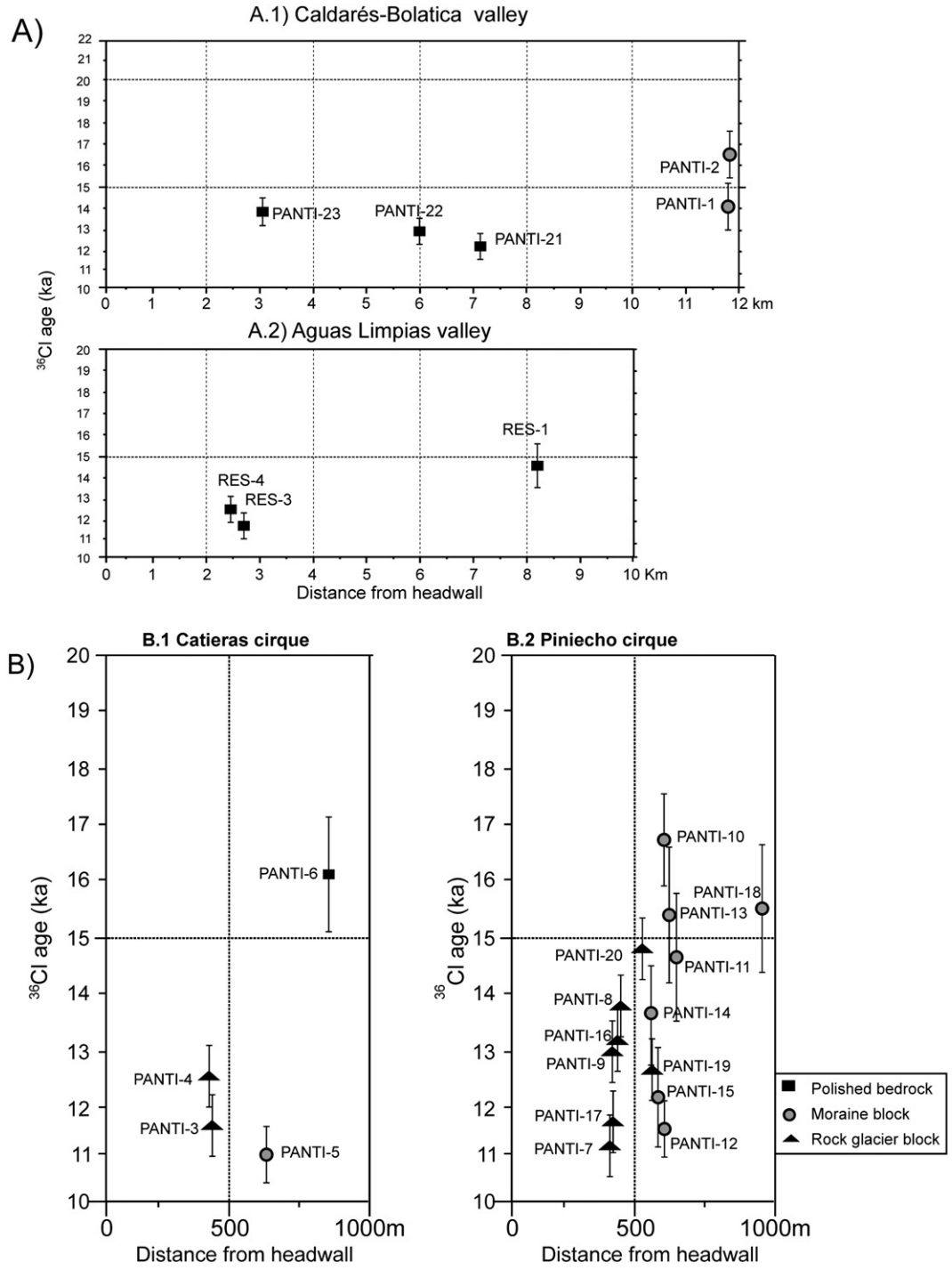

Figure 3. Cosmogenic exposure results and their distribution in relation to distance from the head of the valley. A.1) Caldarés and Bolatica valley; A.2) Aguas Limpias valley; B.1) Catieras Cirque; and B.2) Piniecho Cirque.

There are other deposits within the Piniecho cirque. For instance, an alluvial fan and a large debris flow are present in the northern part of the cirque, perhaps related to the collapse of a moraine ridge. The headwall of the central cirque is affected by numerous debris flows and their corresponding levees, and the cirque and valley walls are covered with screes that are still active.

There are fewer glacial features in the Catieras Cirque (Fig. 10). A small rock glacier 200-m in length is derived from the western headwall. Two blocks sampled in the front of the glacier (PANTI-3 and PANTI-4) yielded a ^{36}Cl minimum exposure ages of 12.5 ± 1.3 ka and 11.6 ± 1.4 ka, indicating that it is similar in age to the rock glaciers in the Piniecho Cirque. A block of small moraine close to the rock glacier (PANTI-5) yielded a ^{36}Cl minimum exposure age of 10.9 ± 1.2 ka. A rocky threshold with a well-preserved glacial polish (PANTI-6), located 100 m below the rock glacier yielded an age of 15.9 ± 1.6 ka.

In summary, the glacial dates obtained from the Piniecho and Catieras cirques are consistent with those obtained from the Aguas Limpias and Caldarés valleys. The moraines that delimited this advance appear to be somewhat younger than the thresholds, probably because of the time involved in the moraine reaching complete stabilization. A later retreat culminated at approximately 14 ka ago, and there were subsequent small local advances near the cirque headwall. These glacial

https://doi.org/10.1016/j.yqres.2015.01.010 Published online by Cambridge University Press

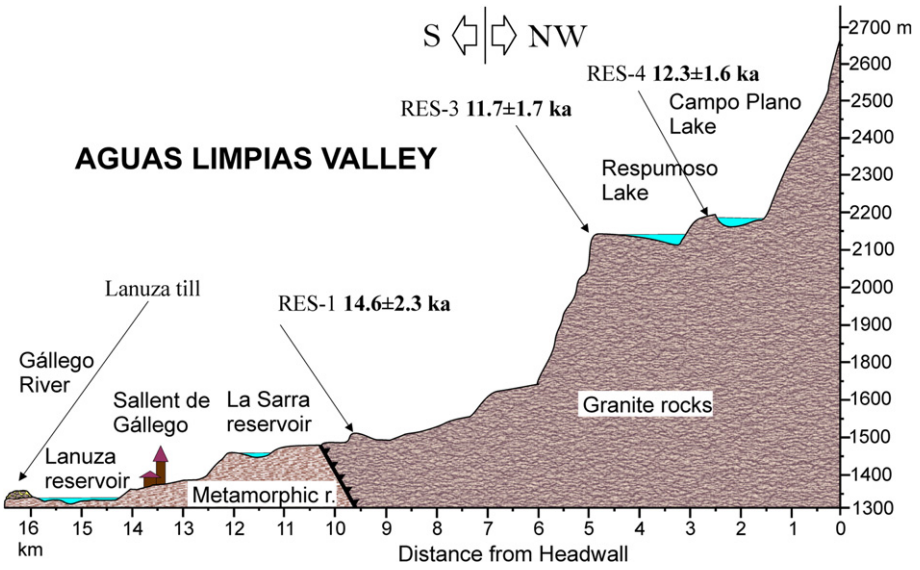

Figure 4. The Aguas Limpias Valley transect and the distribution of cosmogenic exposure results on polished bedrock surfaces.

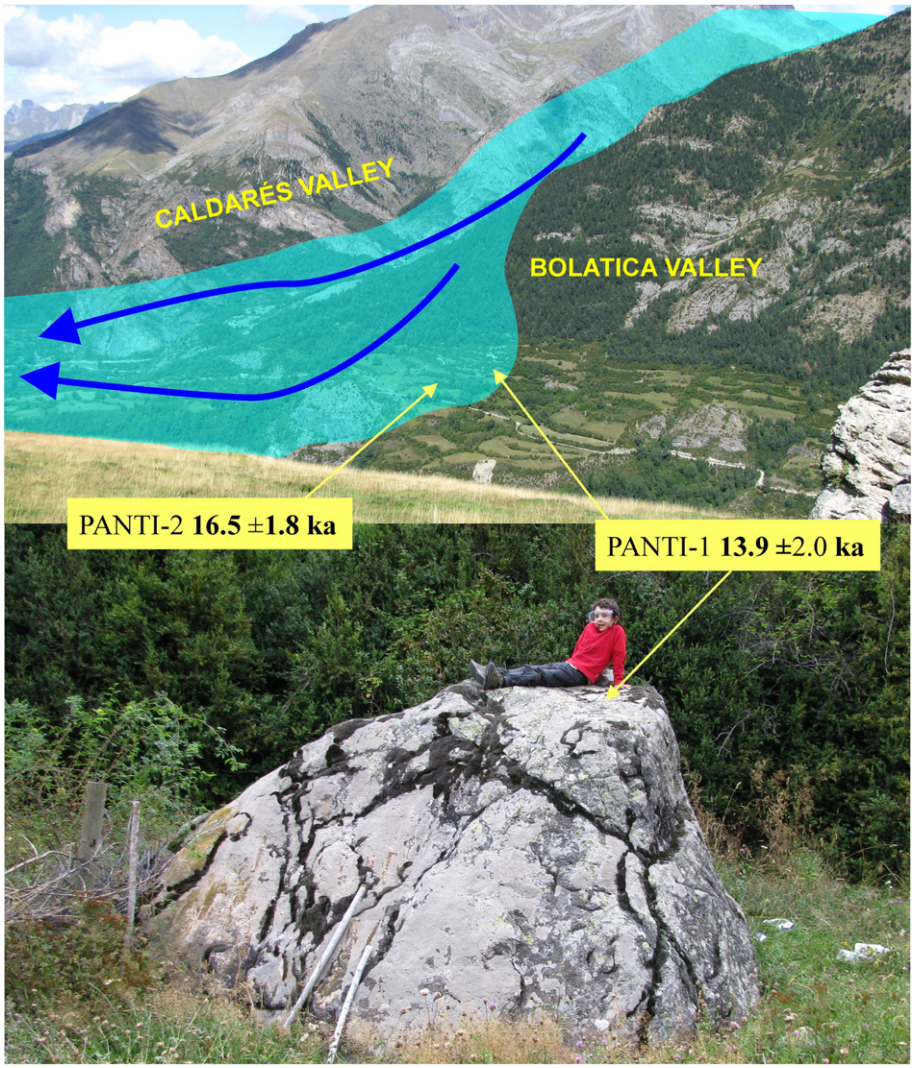

Figure 5. Penetration of the Caldarés Oldest Dryas lateral moraine into the Bolatica Valley, and the boulder corresponding to the PANTI-1 sampling point.

https://doi.org/10.1016/j.yqres.2015.01.010 Published online by Cambridge University Press

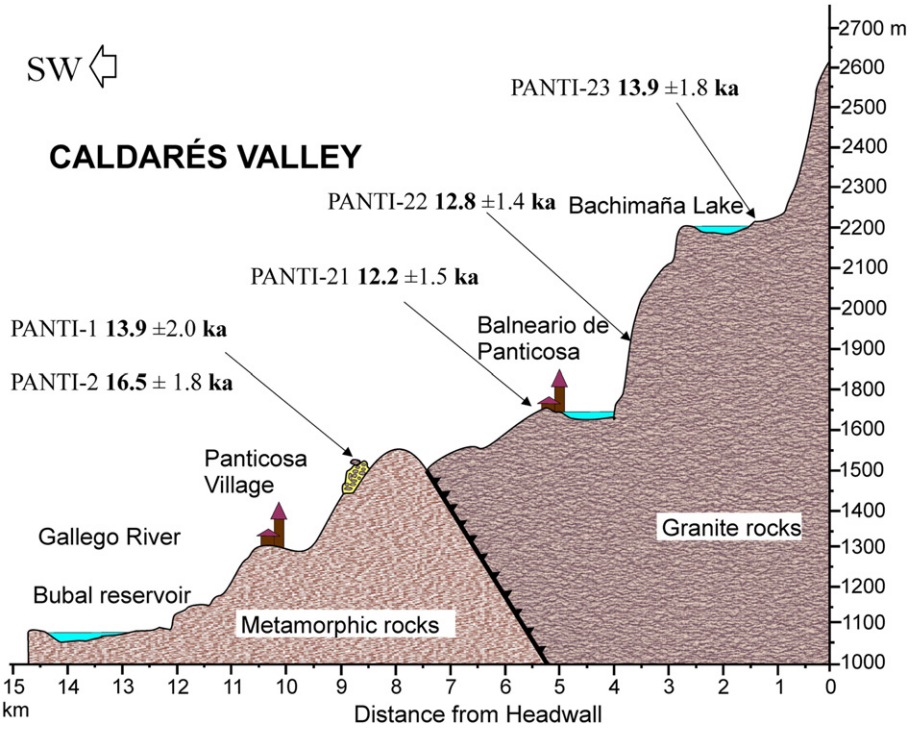

Figure 6. The Caldarés Valley transect, showing the cosmogenic exposure dates for polished bedrock surfaces.

advances were contemporaneous with the development of rock glaciers. The minimum ages determined for these moraines were approximately 11 ka. No evidence of new glacial advances or rock glacier development since 11 ka has been found, except for some cases related to the LIA.

Discussion

A number of studies have revealed the location of most of the end and lateral moraines in the main valleys of the central–southern Pyrenees, particularly the Aragón (García-Ruiz et al., 2013), Aragón Subordán (García-Ruiz and Martí-Bono, 2011), Cinca (Lewis et al., 2009), Gállego (Barrère, 1966; Peña et al., 2003; Lewis et al., 2009; García-Ruiz et al., 2011), and Noguera Ribagorzana and Carol (Pallàs et al., 2006, 2010) valleys. It is noteworthy that the MIE end moraines and their corresponding fluvial terraces have been dated as belonging to the MIS 4 and MIS 3. Similar findings have been reported for other localities in northern Spain, particularly the Cantabrian Range (Moreno et al., 2010b; Frochoso et al., 2013; Jiménez-Sánchez et al., 2013; Serrano et al., 2013). This is consistent with other chronologies reported for certain Mediterranean mountains (Hughes et al., 2006; Hughes and Woodward, 2008). In the case of the central–southern Pyrenees, few clear manifestations of the global LGM have been found, although some indirect results obtained from fluvial terraces, stratified screes and glacio-lacustrine sediments confirm a glacial advance at approximately 20–22 ka, but of consistently lesser extent than the local MIE.

This study focused on deglaciation processes in the upper Gállego Valley, using exposure ages from granitic moraine boulders and polished bedrock. The results highlight the occurrence of several climatic pulses since the global LGM, and the sensitivity of small glaciers to climate variability. The dating method used enabled us, in most cases, to correlate distinct age groups of glacial deposits and thresholds, and to broadly identify some of the main glacial events during the complex period of deglaciation.

Cosmogenic dating methods, based on the cosmogenic isotope ^{10}Be, have previously been used in the study of glacial evolution in the Pyrenees, including in other valleys of the central–southern sector (Pallàs et al., 2006), in the southeastern sector (Delmas et al., 2008; Pallàs et al., 2010) and in the northeastern sector (Delmas et al., 2011). The main difficulty in comparing the results of these studies with those of the present study lies in differences in the snow cover depth and duration: in some cases in the earlier studies an absence of snow cover was assumed, even for samples taken near the summit (Pallàs et al., 2006, 2010), and in other cases a uniform snow cover was assumed (50 cm during 6 months), regardless of the altitude (Delmas et al., 2008, 2011). This is important because the ages obtained from exposure to cosmogenic radiation can vary up to 15% based on the snow cover conditions assumed (Benson et al., 2004; Schildgen et al., 2005; Ivy-Ochs et al., 2009; Böhlert et al., 2011; Stroeven et al., 2011; Hippe et al., 2014). In spite of these limitations, our results are consistent with others based on cosmogenic methods in the Pyrenees.

The interpretation of the results of this work was limited, at the millennial-age resolution, by the geologic scatter in the different deposits and the relatively large age error. We considered all factors that could affect the results, except large post-glacial erosion and cosmogenic inheritance. Both these factors were minimized by sampling polished thresholds, which have experienced high sub-glacial erosion at the bottom of the valleys, preserving the original glacially scoured surface thus minimizing inheritance. However, these factors could be important in morainic blocks, particularly those at the bottom of valleys, including the Bolatica Valley (samples PANTI-1 and PANTI-2), which have been subjected to extensive post-glacial erosion. In addition, it is necessary to add the time involved in moraine stabilization (Putkonen and O'Neal, 2006; Houmark-Nielsen et al., 2012) in estimating absolute ages. Based on its geomorphological position, the same age could be expected for the Lanuza moraine, in the Aguas Limpias Glacier, and based on the threshold ages we assume that by approximately 18–16 ka the ice tongues from the Aguas Limpias and Caldarés valleys had already separated (Fig. 2). This has been referred to as the "disjunction phase" in the glacial evolution of the upper Gállego Valley (Barrère, 1966; Serrano-Cañadas, 1991) or "break up stage" in the eastern and northern Pyrenees (Delmas et al., 2008, 2011).

https://doi.org/10.1016/j.yqres.2015.01.010 Published online by Cambridge University Press

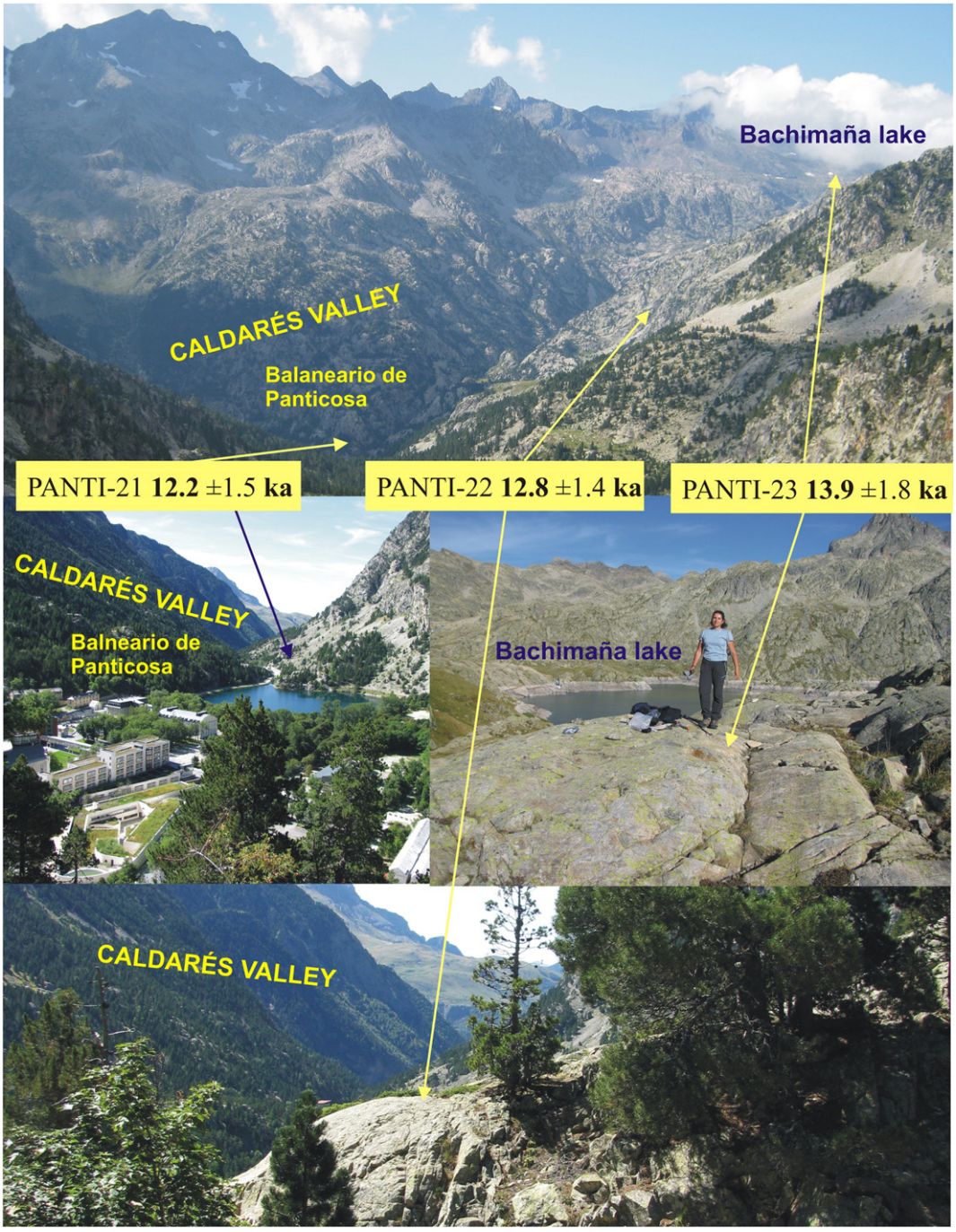

Figure 7. Location and ages for the samples PANTI-21, -22 and -23, from polished bedrock surfaces in the Caldarés Valley.

Similarly, the Gállego Glacier (highest divide not exceeding 2300 m) had retreated to the headwater, and was probably reduced to small ice masses in the cirques (González-Sampériz et al., 2006). For this reason the Aguas Limpias Glacier penetrated into the Gállego Valley, leaving at least two lateral moraine ridges. Previous studies have reported an early deglaciation in the Gállego Valley, particularly the occurrence of deep-seated landslides as a consequence of glacial retreat, which occurred as early as 20,120 ^{14}C cal yr BP (García-Ruiz et al., 2003).

As suggested by indirect evidence, Gállego Glacier expanded during the global LGM, then retreated to the headwater. A new cold period could have represented an advance of 10–12 km for each individual glacier. This left tills at Lanuza and in the lower Caldarés Valley, although the advance was not so great as to result in a new glacial junction. It is noteworthy that evidence of this glacial push has also been detected in the Piniecho Cirque. Using minimum ages for midvalley sites, the rate of retreat to the cirque was relatively rapid (estimated to be approximately 5 km per ka).

The spread in ages and large absolute age error make it difficult to relate this advance to a specific late Pleistocene cold period. Based on correlations with other proxies and the results found, one hypothesis worthy of testing in future research based on expanded sampling is that this period of glacial re-advance is related to the Oldest Dryas (Heinrich Event 1, the Gschnitz Stadial in the Alps, and the "Mystery Interval"; Denton et al., 2006). This was an extremely cold and dry period between approximately 18 and 14.5 ka, when vegetation returned to its glacial state (Clark et al., 2012a), and represents a clear period of

https://doi.org/10.1016/j.yqres.2015.01.010 Published online by Cambridge University Press

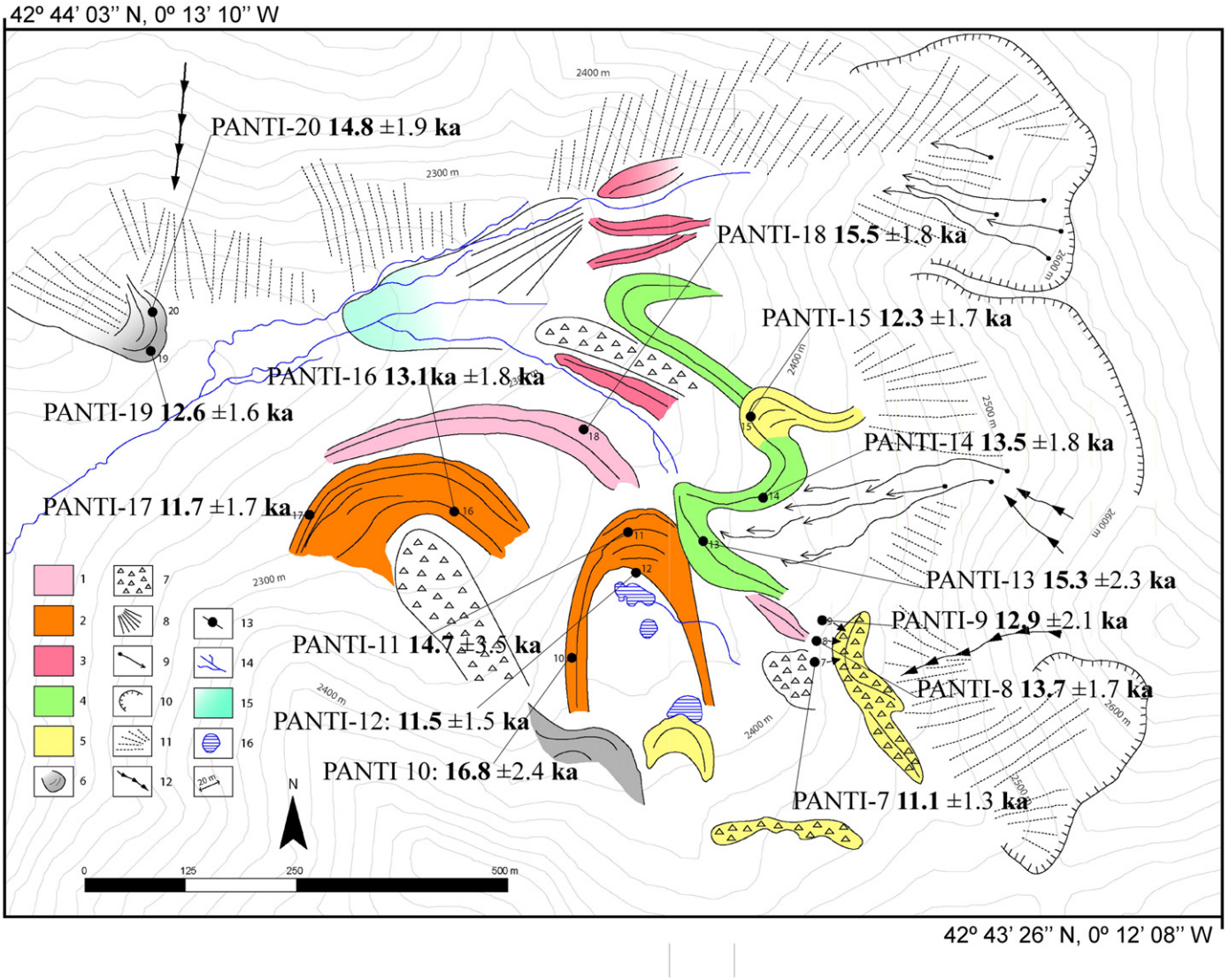

Figure 8. Glacial deposits and other geomorphological features of the Piniecho Cirque. 1–5: Moraine deposits, ordered from the oldest (1) to the youngest (5); 6: Rock glacier; 7: Rock avalanche; 8: Alluvial fan; 9: Debris flows; 10: Glacial cirque; 11: Screes; 12: Rock avalanches; 13: Sampling points; 14: Fluvial network; 15: Sediment accumulation, most likely corresponding to a large hydrological event. 16: Lakes. Distance between contour lines 20 m.

glacial advance following several millennia of retreat. This advance coincided with a very cold and dry period reported for the Mediterranean basin (Dormoy et al., 2009; Fletcher et al., 2010), the Iberian Peninsula (Morellón et al., 2009; González-Sampériz et al., 2013) in lacustrine sediments in the pre-Pyrenees and the Iberian Range, and the Cantabrian Mountains (Pellitero et al., 2011), where rock glaciers developed. In the Alps, precipitation was 1/3 of current levels, and the summer temperature was 10°C lower than now (Ivy-Ochs et al., 2006).

A similar advance during the Oldest Dryas has been reported for southern–central, eastern and northern Pyrenean valleys (Pallàs et al., 2006; Delmas et al., 2008, 2011). Moraines of this period have also been dated in the central (Palacios et al., 2011, 2012a,b) and northwestern Iberian Peninsula (Rodríguez-Rodríguez et al., 2014). The Oldest Dryas moraines are common in many other Mediterranean mountains, including in the Anatolian Peninsula (Sarikaya et al., 2008; Zahno et al., 2010; Akçar et al., 2014), the Balkans (Kuhlemann et al., 2013), the Apennines (Giraudi, 2012) and the Italian Maritime Alps (Federici et al., 2012). In the central Alps the moraines of the Gschnitz Stadial glaciers were formed between 17–16 ka and 15.5 ka (Ivy-Ochs et al., 2006, 2008). Major advances also occurred in this period in the Tatra Mountains (Makos et al., 2013), and almost reached the LGM position in the Scandinavian Ice Sheet (Rinterknecht et al., 2012; Lasberg and Kalm, 2013).

The results appear to indicate that the deglaciation process accelerated at approximately 14 ka, and may be related to Bølling and Allerød interstadials (between approximately 15 and 13.5 ka). This was a period of wetter and warmer climate, which enabled forest expansion in the western Mediterranean (Fletcher et al., 2010). In the study area the polished thresholds were ice-free in the Caldarés Valley upstream of Balneario de Panticosa approximately 12–14 ka. In the Aguas Limpias Valley the ice tongue disappeared from the Respumoso Lake approximately 12 ka, and only small glaciers remained in the headwalls of the divides. Thus, glaciers may have completely disappeared from the cirques, or were reduced to residual ice patches in the headwall, as occurred in the eastern Pyrenees (Delmas et al., 2008, 2011), other northern mountains of the Iberian Peninsula (Fernández-Mosquera et al., 2000; Cowton et al., 2009; Rodríguez-Rodríguez et al., 2011), in the Central Range in central Spain (Palacios et al., 2011, 2012a,b), and in Sierra Nevada, southern Spain (Gómez-Ortiz et al., 2012). In Sierra Nevada the melting of ice masses during the Bølling/Allerød period resulted in the development of rock glaciers that survived until the early Holocene (Palade et al., 2011; Gómez-Ortiz et al., 2012). Marked

https://doi.org/10.1016/j.yqres.2015.01.010 Published online by Cambridge University Press

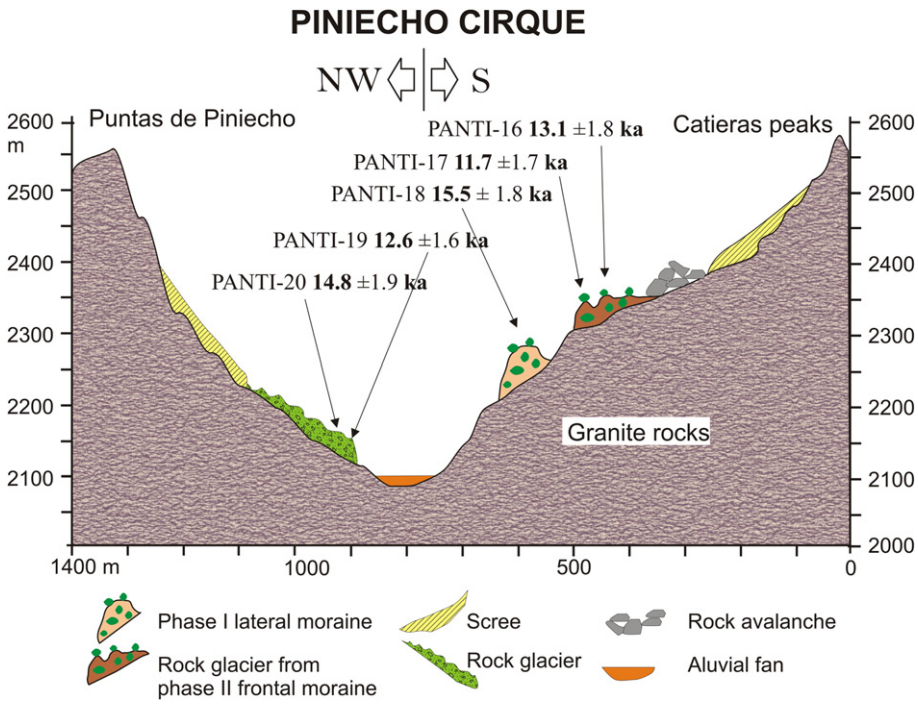

Figure 9. The Piniecho Cirque transect, and the location of the main samples and their cosmogenic exposure ages on various landforms.

downwasting of the alpine glaciers occurred between 14.7 and 12.9 ka (Ivy-Ochs et al., 2006, 2008; Hippe et al., 2014): a similar situation occurred in the Tatra Mountains (Makos et al., 2013) and the Alps (Dielforder and Hetzel, 2014). The Scandinavian Ice Sheet retreated between 14.2 and 13.3 ka (Lasberg and Kalm, 2013), the British-Irish Ice Sheet almost disappeared after 15 ka (Ballantyne, 2010; Clark et al., 2012b; Ballantyne et al., 2013), and the Iceland Ice Sheet broke up catastrophically (Geirsdóttir et al., 2009). In general, there is little information on deglaciation in this period for most Mediterranean mountains, because most attention has been focused on dating moraine blocks, and not polished thresholds. In the Pyrenees, this warm period was characterized by a decrease in the salinity of lakes (Morellón et al., 2009). Nevertheless, the occurrence of a short glacial re-advance in the Piniecho cirque cannot be ruled out. This would be evident through the presence of moraines and rock glaciers, but the age of these could not be determined in this study because of the large error rate. Such a re-advance would correspond to a decline in temperature centered at 14.0 ka, during the Older Dryas. The small rock glaciers in the Piniecho and Catieras valley, which yielded exposure minimum age of 14–13 ka, could belong to the final stage of the Oldest Dryas rather than to the Bølling–Allerød interstadials, or to the short crisis of the Older Dryas.

After the benign period of the Allerød, a relatively sudden temperature decrease (cooling of approximately 5°C; Clark et al., 2012a) and a 30% decline in precipitation (Ivy-Ochs et al., 2006, 2008) resulted in the onset of the Younger Dryas, between approximately 12.9 and 11.7 ka. Glacial advances during the Younger Dryas have also been recorded for other Pyrenean valleys (Pallàs et al., 2006; Delmas et al., 2008, 2011), and for other Mediterranean mountain regions including the Anatolian Peninsula (Akçar et al., 2007, 2014; Zahno et al., 2010), Greek mountains (Hughes et al., 2006), the Balkans (Hughes and Woodward, 2008; Hughes et al., 2010), the Carpathians (Rinterknecht

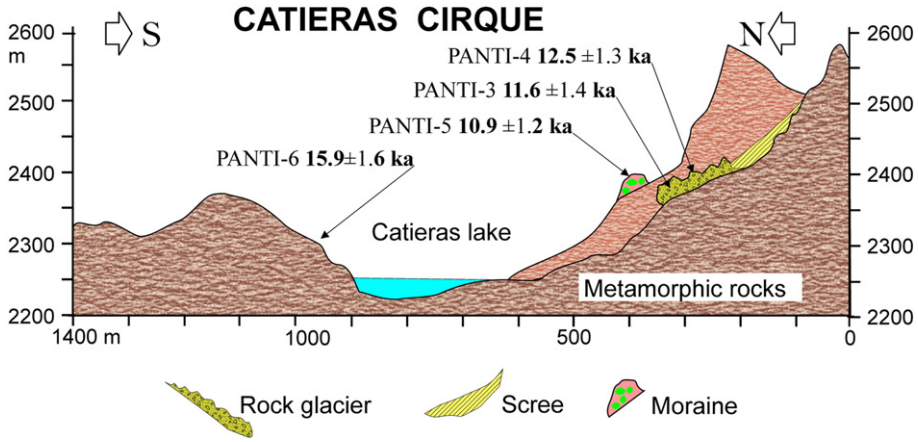

Figure 10. The Catieras Cirque transect, showing the location of the rock glacier, moraine and polished bedrock.

https://doi.org/10.1016/j.yqres.2015.01.010 Published online by Cambridge University Press

et al., 2012), the Maritime Alps (Federici et al., 2012), and the Atlas of Morocco (Hughes et al., 2011). This period was represented by the Egesen Stadial moraines in the Alps (Ivy-Ochs et al., 2006, 2009; Hippe et al., 2014), and by generalized moraine development in many mountain regions and the British–Irish (Ballantyne, 2010) and Scandinavian ice sheets (Rinterknecht et al., 2012; Lasberg and Kalm, 2013).

Nevertheless, in some mountains that were glaciated during most of the late Pleistocene there is no evidence of Younger Dryas moraines (e.g. the Central Ranges, Spain; Palacios et al., 2011, 2012a, 2012b), suggesting that mountains in central Spain were significantly drier than mountains elsewhere in Europe. In some Pyrenean massifs the glacial re-advance was of very limited spatial extent. This occurred for the Marboré Cirque (central–southern Pyrenees), where the Marboré Lake was already deglaciated at 12.7 ka (Oliva-Urcia et al., 2013), despite having a north-facing exposure and being at the foot of a massif exceeding 3200 m asl. Ivy-Ochs et al. (2008) reported that the Younger Dryas was a climatically unstable period, and this perhaps explains the occurrence of several deposits in the Piniecho Cirque, including new moraines and the development of rock glaciers. During the Younger Dryas, glaciers in the Aguas Limpias Valley were confined to ice tongues up to 2 km in length, and these had begun to retreat by approximately the end of this period (11.7 ka).

The occurrence of a small deposit at the foot of the southern cirque in the Piniecho Valley suggests the occurrence of a late cool event that ended approximately 11 ka ago, resulting in the development of a protalus lobe built by rock avalanches. It comprises large blocks and boulders arranged in a chaotic manner with no fine matrix, and thus its structure is very different from the other deposits in the area. The presence of arcs indicates an incipient trend towards a rock glacier, suggesting that it could be the last manifestation of the Younger Dryas. The position and characteristics of the deposit are similar to that of many other glacial deposits located close to cirque headwalls throughout the central–southern Pyrenees; these are usually attributed to the Younger Dryas or to the last cooling of the late Pleistocene (Serrano-Cañadas, 1995, 1998; García-Ruiz et al., 2011). Up to now there has been no evidence of glacial activity during the so-called 10.8 event, which is a short cold period detected in the Alps, and represents the earliest Holocene (Ivy-Ochs et al., 2009).

The results of this study demonstrate that glacial advances and the development of rock glaciers ceased at the end of the Younger Dryas. In the Aguas Limpias Valley the threshold that deglaciated at the end of this period (11.7 ka) is located near the LIA moraines. In the Piniecho and Cateras cirques, the most recent moraine deposits are dated at 11 ka. No new glacial activity has been recorded in the upper Gállego Valley until the LIA.

Conclusions

The current study of deglaciation in the upper Gállego Valley provides the first information for this area on the main stages of glacial advance and retreat between the LGM and the beginning of the Holocene. The results indicate that the sequence of events during deglaciation was similar to that recorded since the LGM in other European mountains. Most previous studies have focused on the location and dating of glacial deposits related to the local MIE and the global LGM. This study has demonstrated:

(i) The rapidity of glacial retreat since the LGM. Although the exact location of the end moraines and the maximum extent of the Gállego Glacier during the LGM were not determined, the occurrence of the LGM was deduced from analysis of glaciolacustrine and proglacial deposits. The glacier later retreated towards the headwater prior to several re-advances and retreats during the late glacial period.

(ii) The sensitivity of small glaciers to climate variability. Mapping and dating of late Glacial deposits in the upper Gállego Valley confirmed that the ice tongues reacted rapidly and extensively to any climate change, causing the deposition of a variety of tills. The spatial distribution and dating of moraines over a short distance within the Piniecho Cirque suggests the occurrence of distinct stages of glacial advance and retreats between 16 and 11 ka, covering the Oldest Dryas and the Younger Dryas periods.

(iii) The occurrence of several climate and glacial reversals from cirque rockwalls or stillstands within a general scenario of deglaciation following the LGM.

(iv) Glacial retreat following the LGM represented the dissociation of ice tongues in the upper Gállego Valley. A new advance occurred before approximately 17 ka, which represented a clear period of glacial expansion involving the deposition of tills in the Aguas Limpias and Caldarés valleys, although they were not again in contact. The Gállego Glacier remained in the headwater. The large error rate associated with the results precludes correlation of this advance with a specific glacial period, but one hypothesis is that it is related to the Oldest Dryas.

(v) Glaciers seem to have advanced again at approximately 14–11.7 ka, although again, exposure age scatter and large age error prevented greater specificity; one hypothesis is that this period is correlated to the Older and Younger Dryas periods. No evidence of glacial re-advances from the Holocene until the Little Ice Age has been found in this area.

(vi) Using minimum ages for midvalley sites, the rate of retreat to cirque headwalls was estimated to be relatively rapid (approximately 5 km per ka).

(vii) During the late glacial advances, small glaciers and rock glaciers developed close to the cirque headwalls, and co-occurred under the same climatic conditions; many of the rock glaciers represent the last phase of glacial decay.

Future studies should focus on locating the end position of the glaciers during the global LGM, which will enable the significance of glacial retreat prior to the onset of the Mystery Interval to be assessed. Detailed mapping and dating of glacial deposits close to the cirques will provide more precise information on glacial reversals during the Oldest and Younger Dryas, and the possibility that re-advance occurred during the Older Dryas.

Acknowledgments

This study was performed with the support of the projects CGL2006-11619/HID, CGL2011-27753-C02-01 and CGL2012-35858, funded by the Spanish Ministry of Economy and Competitiveness. The research group on Geomorphology and Global Change was financed by the Aragón Government and the European Social Found (ESF-FSE) (E68). The authors acknowledge Dr David Fink, Dr Magali Delmas and an anonymous reviewer for their valuable comments on the manuscript. We also particularly thank Dr Irene Schimmelpfennig, whose collaboration was essential to the study.

Appendix A. Supplementary data

Supplementary data to this article can be found online at http://dx.doi.org/10.1016/j.yqres.2015.01.010.

References

Akçar, N., Yavuz, V., Ivy-Ochs, S., Kubik, P.W., Varder, M., Schlüchter, C., 2007. Paleoglacial records from Kavron Valley, NE Turkey: field and cosmogenic exposure dating evidence. Quaternary International 164–165, 170–183.

Akçar, N., Yavuz, V., Ivy-Ochs, S., Reber, R., Kubik, P.W., Zahno, C., Schlüchter, C., 2014. Glacier response to the change in atmospheric circulation in the eastern Mediterranean during the Last Glacial Maximum. Quaternary Geochronology 19, 17–41.

Bakalowicz, M., Sarriaux, P., Ford, D.C., 1984. Quaternary glacial events in the Pyrenees from U-series dating of speleothems in the Niaux–Lombrives–Sabart caves, Ariège, France. Norsk Geografisk Tidsskrift 38, 193–197.
Ballantyne, C.K., 2010. Extent and deglacial chronology of the last British-Irish Ice Sheet: implications for exposure dating using cosmogenic isotopes. Journal of Quaternary Science 25, 515–534.
Ballantyne, C.K., Rinterknecht, V., Gheorghiu, D.M., 2013. Deglaciation chronology of the Galloway Hills Ice Centre, southwest Scotland. Journal of Quaternary Science 28, 412–420.
Barrère, P., 1966. La morphologie quaternaire de la region de Biescas et de Sabiñánigo (Haut Aragón). Bulletin de l'Association Française pour l'Étude du Quaternaire 2, 83–93.
Benson, L., Madole, R., Phillips, W., Landis, G., Thomas, T., Kubik, P., 2004. The probable importance of snow and sediment shielding on cosmogenic ages of north-central Colorado Pinedale and pre-Pinedale moraines. Quaternary Science Reviews 23, 193–206.
Böhlert, R., Egli, M., Maisch, M., Brandová, D., Ivy-Ochs, S., Kubik, P.W., Haeberli, W., 2011. Application of a combination of dating techniques to reconstruct the Lateglacial and Early Holocene landscape history of the Albula region (eastern Switzerland). Geomorphology 127, 1–13.
Bowen, D.Q., Phillips, F.M., McCabe, A.M., Knutz, P.C., Sykes, G.A., 2002. New data for the Last Glacial Maximum in Great Britain and Ireland. Quaternary Science Reviews 21, 89–101.
Brugger, K.A., 2007. Cosmogenic ^{10}Be and ^{36}Cl ages from Late Pleistocene terminal moraine complexes in the Taylor River drainage basin, central Colorado, USA. Quaternary Science Reviews 26, 494–499.
Calle, M., Sancho, C., Peña, J.L., Cunha, P., Oliva-Urcia, B., Pueyo, E., 2013. La secuencia de terrazas cuaternarias del río Alcanadre (provincial de Huesca): caracterización y consideraciones paleoambientales. Cuadernos de Investigación Geográfica 39 (1), 159–178.
Calvet, M., Delmas, M., Gunnell, Y., Braucher, R., Bourlès, D., 2011. Recent advances in research on Quaternary glaciations in the Pyrenees. In: Ehlers, J., Gibbart, P.L., Hughes, P. (Eds.), Quaternary glaciations, extent and chronology. Elsevier, Amsterdam, pp. 127–139.
Chueca, J., Peña Monné, J.L., Lampre, F., García-Ruiz, J.M., Martí-Bono, C., 1998. Los glaciares del Pirineo aragonés: Estudio de su evolución y extension actual. Departamento de Geografía. Universidad de Zaragoza, Zaragoza (104 pp.).
Clark, P.U., Shakun, J.D., Baker, P.A., Bartlein, P.J., Brewer, S., Brook, E., Carlson, A.E., Cheng, H., Kaufman, D.S., Liu, Z., Marchitto, T.M., Mix, A.C., Morrill, C., Otto-Bliesner, B.L., Pahnke, K., Russell, J.M., Whitlock, C., Adkins, J.F., Blois, J.L., Clark, J., Colman, S.M., Curry, W.B., Flower, B.P., He, F., Johnson, T.C., Lynch-Stieglitz, J., Markgraf, V., McManus, J., Mitrovica, J.X., Moreno, P.I., Williams, J.W., 2012a. Global climate evolution during the last deglaciation. PNAS 109 (19), E1134–E1142.
Clark, C.D., Hughes, A.L.C., Greenwood, S.L., Jordan, C., Sejrup, H.P., 2012b. Pattern and timing of retreat of the last British-Irish Ice Sheet. Quaternary Science Reviews 44, 112–146.
Combourieu-Nebout, N., Peyron, O., Desprat, S., Beaudouin, C., Kotthoff, U., Marret, F., 2009. Rapid climatic variability in the west Mediterranean during the last 25 000 years from high resolution pollen data. Climate of the Past 5, 503–521.
Cowton, T., Hughes, P.D., Gibbard, P.L., 2009. Palaeoglaciation of Parque Natural Lago de Sanabria, Northwest Iberia. Geomorphology 108, 282–291.
CRONUS-Earth Project, 2014. http://web1.ittc.ku.edu:8888/html/latest/topo/ (accessed in August 2014).
Darnault, R., Rolland, Y., Braucher, R., Bourlès, D., Revel, M., Sánchez, G., Bouissou, S., 2012. Timing of the last deglaciation revealed by receding glaciers in the Alpine-scale: impact on mountain geomorphology. Quaternary Science Reviews 31 (12), 127–142.
de la Riva, J., 2000. Caracterización climática del alto valle de Tena. Boletín Glaciológico Aragonés 1, 81–109.
Delmas, M., 2005. La déglaciation dans le massif du Carlit (Pyrénées orientales): approaches géomorphologique et géochronologique nouvelles. Quaternaire 16, 45–55.
Delmas, M., 2009. Chronologie et impact géomorphologique des glaciations quaternaires dans l'est des Pyrénées. Thèse Doctorat Université de Paris I (unpublished), 523 pp.
Delmas, M., Gunnell, Y., Braucher, R., Calvet, M., Bourlès, D., 2008. Exposure age chronology of the last glaciation in the eastern Pyrenees. Quaternary Research 69, 231–241.
Delmas, M., Calvet, M., Gunnell, Y., Braucher, R., Bourlès, D., 2011. Palaeogeography and 10Be exposure-age chronology of Middle and Late Pleistocene glacier systems in the northern Pyrenees: implications for reconstructing regional palaeoclimates. Palaeogeography, Palaeoclimatology, Palaeoecology 305, 109–122.
Delmas, M., Calvet, M., Gunnell, Y., Braucher, R., Bourlès, D., 2012. Les glaciations quaternaires dans les Pyrénées ariégeoises: approche historiographique, données paleogéographiques et chronologies nouvelles. Quaternaire 23, 61–85.
Denton, G.H., Broecker, W.S., Alley, R.B., 2006. The mystery interval 17.5 to 14.5 kyrs ago. PAGES News 14 (20), 14–16.
Desilets, D., Zreda, M., Almasi, P.F., Elmore, D., 2006. Determination of cosmogenic Cl-36 in rocks by isotope dilution: innovations, validation and error propagation. Chemical Geology 233, 185–195.
Dielforder, A., Hetzel, R., 2014. The deglaciation history of the Simplon region (southern Swiss Alps) constrained by 10Be exposure dating of ice-molded bedrock surfaces. Quaternary Science Reviews 84, 26–38.
Dormoy, I., Peyron, O., Combourieu Nebot, N., Goring, S., Kotthoff, U., Magny, M., Pross, J., 2009. Terrestrial climate variability and seasonality changes in the Mediterranean region between 15 000 and 4000 years BP deduced from marine pollen records. Climate of the Past 5, 615–632.
Federici, P.R., Granger, D.E., Riobolini, A., Spagnolo, M., Pappalardo, M., Cyr, A.J., 2012. Last glacial maximum and the Gschnitz stadial in the Maritime Alps according to ^{10}Be cosmogenic dating. Boreas 41, 277–291.
Fernández-Mosquera, D., Marti, K., Vidal-Romaní, J.R., Weigel, A., 2000. Late Pleistocene deglaciation chronology in the NW of the Iberian Peninsula using cosmicray produced 21 Ne in quartz. Nuclear Instruments and Methods in Physics Research B172, 832–837.
Fink, D., Vogt, S., Hotchkis, M., 2000. Cross-sections for ^{36}Cl from Ti at Ep = 35–150 MeV: applications to in-situ exposure dating. Nuclear Instruments and Methods in Physics Research Section B: Beam Interactions with Materials and Atoms 172, 861–866.
Fletcher, W.J., Sánchez Goñi, M.F., Peyron, O., Dormoy, I., 2010. Abrupt climate changes of the last deglaciation detected in a Western Mediterranean forest record. Climate of the Past 6, 245–264.
Frochoso, M., González-Pellejero, R., Allende, F., 2013. Pleistocene glacial morphology and timing of Last Glacial Cycle in Cantabrian Mountains (Northern Spain): new chronological data from the Asón area. Central European Journal of Geosciences 5, 12–27.
García-Ruiz, J.M., Martí-Bono, C., 2002. Mapa geomorfológico del Parque Nacional de Ordesa y Monte Perdido. Ministerio de Medio Ambiente, Madrid (106 pp.).
García-Ruiz, J.M., Martí-Bono, C., 2011. Los depósitos glaciares del valle del Aragón Subordán, Pirineo Centro-occidental español. Cuaternario y Geomorfología 25, 57–81.
García-Ruiz, J.M., Gómez-Villar, A., Ortigosa, L., Martí-Bono, C., 2000. Morphometry of glacial cirques in the Central Spanish Pyrenees. Geografiska Annaler 82A, 433–442.
García-Ruiz, J.M., Valero-Garcés, B., González-Sampériz, P., Lorente, A., Martí-Bono, C., Beguería, S., Edwards, L., 2001. Stratified scree in the Central Spanish Pyrenees: palaeoenvironmental implications. Permafrost and Periglacial Processes 12, 233–242.
García-Ruiz, J.M., Valero-Garcés, B.L., Martí-Bono, C., González-Sampériz, P., 2003. Asynchroneity of maximum glacier advances in the central Spanish Pyrenees. Journal of Quaternary Science 18, 61–72.
García-Ruiz, J.M., Peña-Monné, J.L., Martí-Bono, C., Gómez-Villar, A., Constante Orrios, A., Espinalt-Brillas, M., 2011. El relieve del Alto Aragón occidental. Cartografía y síntesis geomorfológica. Publicaciones del Consejo de Protección de la Naturaleza de Aragón, Zaragoza (91 pp.).
García-Ruiz, J.M., Martí-Bono, C., Peña-Monné, J.L., Sancho, C., Rhodes, E.J., Valeero-Garcés, B., González-Sampériz, P., Moreno, A., 2013. Glacial and fluvial deposits in the Aragón Valley, central-western Pyrenees: chronology of the Pyrenean Late Pleistocene glaciers. Geografiska Annaler, Series A, Physical Geography 95, 15–32.
Geirsdóttir, Á., Miller, G.H., Axford, Y., Olafsdottir, S., 2009. Holocene and latest Pleistocene climate and glacier fluctuations in Iceland. Quaternary Science Reviews 28, 2107–2118.
Giraudi, C., 2012. The Campo Felice Late Pleistocene glaciation (Apennines, Central Italy). Journal of Quaternary Science 27 (4), 432–440.
Gómez-Ortiz, A., Palacios, D., Palade, B., Vázquez-Selem, L., Salvador_Franch, F., 2012. The deglaciation of Sierra Nevada (Southern Spain). Geomorphology 159–160, 93–105.
González-Sampériz, P., Valero-Garcés, B.L., Moreno, A., Jalut, G., García-Ruiz, J.M., Martí-Bono, C., Delgado-Huertas, A., Navas, A., Otto, T., Dedoubat, J.J., 2006. Climate variability in the Spanish Pyrenees during the last 30,000 yr revealed by the El Portalet sequence. Quaternary Research 66, 38–52.
González-Sampériz, P., García-Prieto, E., Aranbarri, J., Valero-Garcés, B.L., Moreno, A., Gil-Romera, G., Sevilla-Callejo, M., Santos, L., Morellón, M., Mata, P., Andrade, A., Carrión, J.S., 2013. Reconstrucción paleoambiental del último ciclo glacial–interglacial en la Iberia continental: la secuencia del Cañizar de Villarquemado (Teruel). Cuadernos de Investigación Geográfica 39 (1), 49–76.
Gosse, J.C., Phillips, F.M., 2001. Terrestrial in situ cosmogenic nuclides: theory and application. Quaternary Science Reviews 20, 1475–1560.
Guerrero, J., Gutiérrez, F., Carbonel, D., Bonachea, J., García-Ruiz, J.M., Galve, J.P., Lucha, P., 2013. 1:5000 landslide map of the upper Gállego Valley (central Spanish Pyrenees). Journal of Maps 8, 484–491.
Hippe, K., Ivy-Ochs, S., Kober, F., Zasadni, J., Wieler, R., Wacker, L., Kubik, P.W., Schlüchter, C., 2014. Chronology of Lateglacial ice flow reorganization and deglaciation in the Gotthard Pass area, Central Swiss Alps, based on cosmogenic ^{10}Be and in situ ^{14}C. Quaternary Geochronology 19, 14–26.
Houmark-Nielsen, M., Linge, H., Fabel, D., Schnabel, C., Xu, S., Wilcken, K.M., Binnie, S., 2012. Cosmogenic surface exposure dating the last glaciation in Denmark: discrepancies with independent age constraints suggests delayed periglacial landform stabilization. Quaternary Geochronology 13, 1–17.
Hughes, P.D., Woodward, J.C., 2008. Timing of glaciation in the Mediterranean mountains during the last cold stage. Journal of Quaternary Science 23, 575–588.
Hughes, P.D., Woodward, J.C., Gibbard, P.L., 2006. Glacial history of the Mediterranean mountains. Progress in Physical Geography 30, 334–364.
Hughes, P.D., Woodward, J.C., Van Calteren, P.C., Thomas, L.E., Adamson, K.R., 2010. Pleistocene ice caps in the coastal mountains of the Adriatic Sea. Quaternary Science Reviews 29, 3690–3708.
Hughes, P.D., Fenton, C.R., Gibbard, P.L., 2011. Quaternary glaciations of the Atlas Mountains, North Africa. In: Ehlers, J., Gibbard, P.L., Hughes, P.D. (Eds.), Quaternary glaciations—Extent and chronology: A closer look. Developments in Quaternary Science 15. Elsevier, Amsterdam, pp. 1065–1074.
Ivy-Ochs, S., Schäffer, J., Kubik, P.W., Synal, H.N., Schlüchter, C., 2004a. Timing of deglaciation on the northern Alpine foreland (Switzerland). Eclogae Geologicae Helvetiae 97, 47–55.
Ivy-Ochs, S., Synal, H.A., Roth, C., Schaller, M., 2004b. Initial results from isotope dilution for Cl and Cl-36 measurements at the PSI/ETH Zurich AMS facility. Nuclear Instruments and Methods in Physics Research Section B: Beam Interactions with Materials and Atoms 223–224, 623–627.

https://doi.org/10.1016/j.yqres.2015.01.010 Published online by Cambridge University Press

Ivy-Ochs, S., Kerschner, H., Kubik, P., Schlüchter, C., 2006. Glacier response in the European Alps to Heinrich Event 1 cooling: the Gschnitz stadial. Journal of Quaternary Science 21, 115–130.
Ivy-Ochs, S., Kerschner, H., Reuther, A., Preusser, F., Heine, K., Masich, M., Kubik, P.W., Schlüchter, C., 2008. Chronology of the last glacial cycle in the European Alps. Journal of Quaternary Science 23, 559–573.
Ivy-Ochs, S., Kerschner, H., Maisch, M., Christl, M., Kubik, P.W., 2009. Latest Pleistocene and Holocene glacier variations in the European Alps. Quaternary Science Reviews 28, 2137–2149.
Jalut, G., Montserrat, J., Fontugne, M., Delibrias, G., Vilaplana, J.M., Julià, R., 1992. Glacial to interglacial vegetation changes in the northern and southern Pyrenees: deglaciation, vegetation cover and chronology. Quaternary Science Reviews 11, 449–480.
Jiménez-Sánchez, M., Rodríguez-Rodríguez, L., García-Ruiz, J.M., Domínguez-Cuesta, M.J., Farias, P., Valero-Garcés, B., Moreno, A., Rico, M., Valcárcel, M., 2013. A review of glacial geomorphology and chronology in northern Spain: timing and regional variability during the last glacial cycle. Geomorphology 196, 50–64.
Julián, A., Chueca, J., Peña, J.L., 2000. El relieve del Alto Gállego (Pirineo aragonés). Boletín Glaciológico Aragonés 1, 45–79.
Kerschner, H., Ivy-Ochs, S., 2008. Paleoclimate from glaciers: examples from the Eastern Alps during the Alpine Lateglacial and early Holocene. Global and Planetary Change 60, 58–71.
Kuhlemann, J., Gachev, E., Gikov, A., Nedkov, S., Krumrei, I., Kubik, P., 2013. Glaciation in the Rila Mountains (Bulgaria) during the Last Glacial Maximum. Quaternary International 293, 51–62.
Lasberg, K., Kalm, V., 2013. Chronology of Late Weichselian glaciation in the western part of the East European Plain. Boreas 42, 995–1007.
Lenton, T.M., 2011. Early warning of climate tipping points. Nature Climate Change 1, 201–209. http://dx.doi.org/10.1038/NCLIMATE1143.
Lewis, C.J., McDonald, E.V., Sancho, C., Peña, J.L., Rhodes, E.J., 2009. Climatic implications of correlated Upper Pleistocene glacial and fluvial deposits on the Cinca and Gállego Rivers (NE Spain) based on OSL dating and soil stratigraphy. Global and Planetary Change 67, 141–152.
López-Moreno, J.I., 2000. Los glaciares del alto valle del Gállego (Pirineo Central) desde la Pequeña Edad del Hielo. Implicaciones en la evolución de la temperatura. Geoforma Ediciones, Logroño (77 pp.).
López-Moreno, J.I., 2005. Recent variations of snowpack depth in the Central Spanish Pyrenees. Arctic, Antarctic and Alpine Research 37, 253–260.
Lopez-Moreno, J.I., Goyette, S., Beniston, M., 2009. Impact of climate change on snowpack in the Pyrenees: horizontal spatial variability and vertical gradients. Journal of Hydrology 374 (3–4), 384–396.
López-Moreno, J.I., Latron, J., Lehmann, A., 2010. Effects of simple and grid size on the accuracy and stability of regression-bases snow interpolation methods. Hydrological Processes 24, 1914–1928.
López-Moreno, J.I., Pomeroy, J., Revuelto, J., Vicente-Serrano, S.M., 2013. Response of snow processes to climate change: spatial variability in a small basin in the Spanish Pyrenees. Hydrological Processes 27, 2637–2650.
Makos, M., Nitychoruk, J., Zreda, M., 2013. Deglaciation chronology and paleoclimate of the Pieciu Stawów Polskich/Rotzoki Valley, high Tatra Mountains, Western Carpathians, since the Last Glacial Maximum, inferred from ^{36}Cl exposure dating and glacier-climate modelling. Quaternary International 293, 63–78.
Martínez de Pisón, E., Serrano, E., 1998. Morfología glaciar del valle de Tenaq (Pirineo aragonés). In: Gómez-Ortiz, A., Pérez-Alberti, A. (Eds.), Las huellas glaciares de las montañas españolas. Universidade de Santiago de Compostela, Santiago de Compostela, pp. 239–261.
Mix, A.C., Bard, E., Schneider, R., 2001. Environmental processes of the ice age: land, oceans, glaciers (EPILOG). Quaternary Science Reviews 20, 627–657.
Morellón, M., Valero-Garcés, B., Vegas-Villarrúbia, T., González-Sampériz, P., Romero, O., Delgado-Huertas, A., Mata, P., Moreno, A., Rico, M., Corella, J.P., 2009. Lateglacial and Holocene palaeohydrology in the western Mediterranean region: the Lake Estanya record (NE Spain). Quaternary Science Reviews 28, 2582–2599.
Moreno, A., Stoll, H.S., Jiménez-Sánchez, M., Cacho, I., Valero-Garcés, B., Ito, E., Edwards, R.L., 2010a. A speleothem record of glacial (25–11.6 kyr BP) rapid climatic changes from northern Iberian Peninsula. Global and Planetary Change 71, 218–231.
Moreno, A., Valero-Garcés, B.L., Jiménez-Sánchez, M., Domínguez-Cuesta, M.J., Mata, M.P., Navas, A., González-Sampériz, P., Stoll, H., Farias, P., Morellón, M., Corella, J.P., Rico, M., 2010b. The last deglaciation in the Picos de Europa National Park (Cantabrian Mountains, northern Spain). Journal of Quaternary Science 25, 1076–1091.
Moreno, A., González Sampériz, P., Morellón, M., Valero-Garcés, B.L., Fletcher, W.J., 2012. Northern Iberian abrupt climate change dynamics during the last glacial cycle: a view from lacustrine sediments. Quaternary Science Reviews 36, 139–153.
Oliva-Urcia, B., Moreno, A., Valero-Garcés, B., Mata, P., Grupo HORDA, 2013. Magnetismo y cambios ambientales en registros terrestres: el lago de Marboré, Parque Nacional de Ordesa y Monte Perdido (Huesca). Cuadernos de Investigación Geográfica 39 (1), 117–140.
Palacios, D., de Marcos, J., Vázquez-Selem, L., 2011. Last glacial maximum and deglaciation of Sierra de Gredos, central Iberian Peninsula. Quaternary International 233, 16–26.
Palacios, D., de Andrés, N., de Marcos, J., Vázquez-Selem, L., 2012a. Glacial landforms and their paleoclimatic significance in the Sierra de Guadarrama, Central Iberian Peninsula. Geomorphology 139, 67–78.
Palacios, D., Andrés, N., Marcos, J., Vázquez-Selem, L., 2012b. Maximum glacial advance and deglaciation of the Pinar Valley (Sierra de Gredos, Central Spain) and its significance in the Mediterranean context. Geomorphology 177–178, 51–61.
Palade, B., Palacios Estremera, D., Gómez Ortiz, A., 2011. Los glaciares rocosos de Sierra Nevada y su significado paleoclimático. Una primera aproximación. Cuadernos de Investigación Geográfica 37 (2), 95–118.
Pallàs, R., Rodés, Á., Braucher, R., Carcailler, J., Ortuño, M., Bordonau, J., Bourlès, D., Vilaplana, J.M., Masana, E., Santanach, P., 2006. Late Pleistocene and Holocene glaciation in the Pyrenees: a critical review and new evidence from 10Be exposure ages, south-central Pyrenees. Quaternary Science Reviews 25, 2937–2963.
Pallàs, R., Rodés, Á., Braucher, R., Bourlès, D., Delmas, M., Calvet, M., Gunnell, Y., 2010. Small isolated glacial catchments as priority targets for cosmogenic surface exposure dating of Pleistocene climate fluctuations, southeastern Pyrenees. Geology 38, 891–894.
Pellitero, R., Serrano, E., González-Trueba, J.J., 2011. Glaciares rocosos del sector central de la Montaña Cantábrica: indicadores paleoambientales. Cuadernos de Investigación Geográfica 37 (2), 119–144.
Peltier, W.R., Fairbanks, R.G., 2006. Global ice volume and Last Glacial Maximum duration from an extended Barbados sea level record. Quaternary Science Reviews 25, 3322–3337.
Peña, J.L., Sancho, C., Lewis, C., McDonald, E., Rhodes, E., 2003. Las morrenas terminales de los valles glaciares del Gállego y Cinca (Pirineo de Huesca). Datos cronológicos. Boletín Glaciológico Aragonés 4, 91–109.
Phillips, F.M., Zreda, M.G., Gosse, J.C., Klein, J., Evenson, E.B., Hall, R.D., Chadwick, O.A., Sharma, P., 1997. Cosmogenic ^{36}Cl and ^{10}Be ages of Quaternary glacial and fluvial deposits of the Wind River Range, Wyoming. Geological Survey of America Bulletin 109, 1453–1463.
Phillips, F.M., Stone, W.D., Fabryka-Martin, J.T., 2001. An improved approach to calculating low-energy cosmic-ray neutron fluxes near the land/atmosphere interface. Chemical Geology 175, 689–701.
Phillips, F.M., 2003. Cosmogenic ^{36}Cl ages of Quaternary basalt flows in the Mojave Desert, California, USA. Geomorphology 53, 199–208.
Putkonen, J., O'Neal, M., 2006. Degraded unconsolidated Quaternary landforms in the western North America. Geomorphology 75, 408–419.
Quinif, Y., Maire, R., 1998. Pleistocene deposits in Pierre Saint-Martin Cave, French Pyrenees. Quaternary Research 49, 37–50.
Ravazzi, C., Badino, F., Marsetti, D., Patera, G., Reimer, P.J., 2012. Glacial to paraglacial history and forest recovery in the Oglio glacier system (Italian Alps) between 26 and 15 ka cal BP. Quaternary Science Reviews 58, 146–161.
Rinterknecht, V., Braucher, R., Böse, M., Bourlès, D., Mercier, J.-L., 2012. Late Quaternary ice sheet extents in northeastern Germany inferred from surface exposure dating. Quaternary Science Reviews 44, 89–95.
Rodríguez-Rodríguez, L., Jiménez-Sánchez, M., Domínguez-Cuesta, M.J., Rico, M.T., Valero-Garcés, B., 2011. Last deglaciation in NW Spain: new chronological and geomorphic evidence from the Sanabria region. Geomorphology 135, 48–65.
Rodríguez-Rodríguez, L., Jiménez-Sánchez, M., Domínguez-Cuesta, M.J., Rinterknecht, V., Pallàs, R., Bourlès, D., Valero-Garcés, B., 2014. A multiple dating-method approach applied to the Sanabria Lake moraine complex (NW Iberian Peninsula, SW Europe). Quaternary Science Reviews 83, 1–10.
Sarikaya, M.A., Zreda, M., Çiner, A., Zweck, Ch., 2008. Cold and wet Last Glacial Maximum on Mount Sandiras, SW Turkey, inferred from cosmogenic dating and glacier modelling. Quaternary Science Reviews 27 (7–8), 769–789.
Scheffer, M., Carpenter, S., Foley, J.A., Folke, C., Walker, B., 2001. Catastrophic shifts in ecosystems. Nature 413, 591–596.
Schildgen, T.F., Phillips, W.M., Purves, R.S., 2005. Simulation of snow shielding corrections fort cosmogenic nuclide surface exposure studies. Geomorphology 64, 67–85.
Schimmelpfennig, I., 2009. Cosmogenic ^{36}Cl in Ca and K Rich Minerals: Analytical Developments, Production Rate Calibrations and Cross Calibration with ^{3}He and ^{21}Ne. (PhD Thesis). Universite Paul Cezanne Aix-Marseille III, CEREGE, Aix en Provence, France.
Schimmelpfennig, I., Benedetti, L., Finkel, R., Pik, R., Blard, P.H., Bourle, D., Burnard, P., Williams, A., 2009. Sources of in-situ ^{36}Cl in basaltic rocks. Implications for calibration of production rates. Quaternary Geochronology 4, 441–461.
Schimmelpfennig, I., Schaefer, J.M., Putnam, A.E., Koffman, T., Benedetti, L., Ivy-Ochs, S., Aster Team, Schulüchter, Ch., 2014. ^{36}Cl production rate from K-spallation in the European Alps (Chironico landslide, Switzerland). Journal of Quaternary Science 29, 407–413.
Scourse, J.D., Haapaniemi, A.I., Colmenero-Hidalgo, E., Peck, V.L., Hall, I.R., Austin, W.E.N., Knutz, P.C., Zahn, R., 2009. Growth, dynamics and deglaciation of the last British-Irish ice sheet: the deep-sea ice rafted detritus record. Quaternary Science Reviews 28, 3066–3084.
Serrano, E., González-Trueba, J.J., Pellitero, R., González-García, M., Gómez-Lende, M., 2013. Quaternary glacial evolution in the Central Cantabrian Mountains (Northern Spain). Geomorphology 196, 65–82.
Serrano-Cañadas, E., 1991. Glacial evolution of the Upper Gállego Valley (Panticosa mountains and Riberda de Biescas, Aragonese Pyrenees, Spain). Pirineos 138, 83–104.
Serrano-Cañadas, E., 1995. Geomorfología de la Sierra de Tendeñera (Pirineo aragonés). Ería 37, 143–158.
Serrano-Cañadas, E., 1998. Geomorfología del Alto Gállego (Pirineo aragonés). Institución Fernando El Católico, Zaragoza (501 pp.).
Stone, J.O., 2000. Air pressure and cosmogenic isotope production. Journal of Geophysical Research 105 (B10), 23753–23759.
Stone, J.O., Allan, G.L., Fifield, L.K., Cresswell, R.G., 1996. Cosmogenic ^{36}Cl from calcium spallation. Geochimica et Cosmochimica Acta 60 (4), 679–692.
Stone, J.O., Fifield, K., Vasconcelos, P., 2005. Terrestrial chlorine-36 production from spallation of iron. Abstract of 10th International Conference on Accelerator Mass Spectrometry. September 5–10, 2005, Berkeley, USA (http://llnl.confex.com/llnl/ams10/techprogram/P1397.HTM).

https://doi.org/10.1016/j.yqres.2015.01.010 Published online by Cambridge University Press

Stroeven, A.P., Fabel, D., Harbor, J.M., Fink, D., Coffee, M.W., Dahlgren, T., 2011. Importance of sampling across an assemblage of glacial landforms for interpreting cosmogenic ages of deglaciation. Quaternary Research 76, 148–156.
Vermeesch, P., 2007. CosmoCalc: an excel add-in for cosmogenic nuclide calculations. Geochemistry, Geophysics, Geosystems 8, 1525–2027.
Williams, C., Flower, B.P., Hastings, D.W., 2012. Seasonal Laurentide Ice Sheet melting during the "Mystery Interval" (15.5–14.5 ka). Geology 40, 955–958.
Yokoyama, Y., Lambeck, K., De Deckker, P., Johnston, P., Fifield, L.K., 2000. Timing of the Last Glacial Maximum from observed sea-level minima. Nature 406, 713–716.
Zahno, C., Akçar, N., Yavuz, V., Kunik, P.W., Schlüchter, C., 2009. Surface exposure dating of Late Pleistocene glaciations at the Dedegöl Mountains (Lake Beysehir, SW Turkey). Journal of Quaternary Science 24, 1016–1028.
Zahno, C., Akçar, N., Yavuz, V., Kubik, P.W., Schluchter, C., 2010. Chronology of Late Pleistocene glacier variations at the Udulağ Mountain, NW Turkey. Quaternary Science Reviews 29, 1173–1187.
Zreda, M., Enbgland, J., Phillips, F., Elmore, D., Sharma, P., 1999. Unblocking of the Nares Strait by Greenland and Ellesmere ice-sheet retrest 10,000 years ago. Nature 398, 128–142.

https://doi.org/10.1016/j.yqres.2015.01.010 Published online by Cambridge University Press